Performance and membrane fouling of alumina UF membranes in treating nano-sized oil-water emulsions

By

Hao Liu

August 2022

In partial fulfillment of the requirements for the degree of

Master of science

In Civil Engineering

Assessment Committee:	TU Delft	Dr. ir. S.G.J. Heijman
	TU Delft	Prof.dr.ir. L.C. Rietveld
	TU Delft	Dr. ir. Ralph Lindeboom

List of Abbreviations

CMC: Critical micelle concentration

COD: Chemical Oxygen Demand

O/W emulsion: oil in water emulsion

TMP: Trans-membrane pressure

SDS: Sodium dodecyl sulfate

UF: Ultrafiltration

TOC: Total organic carbon

PSD: Particle size distribution

Abstract

Ultrafiltration (UF) is an efficient and effective method of filtrating oil-in-water (O/W) emulsions. However, the favorable conditions of filtrating nano-sized O/W emulsions have not been investigated. This study investigated the influence of four different parameters including membrane pore size, cross flow velocity, pH and salinity on membrane fouling as well as oil rejection. Alumina UF membranes were employed to filtrate nano-sized O/W emulsions. O/W emulsions were synthesized using soybean oil and stabilized by surfactants. The filtration experiments were conducted under constant flux for multi cycles. The results showed that 200nm was recommended to filtrate nano-sized O/W emulsions (average droplet size ~100nm) based on the high oil rejection (95% ~ 99%) and low irreversible fouling resistance. Besides, alumina membranes were proved to be more effective in fouling mitigation at low salinity, high pH, and high cross flow velocities.

Acknowledgement

After two challenging and wonderful life in Delft, my journey in TUD finally came to an end. Here I just want to show my sincere thanks to my teachers, family and friends. First, I want to say thank you to all my committee members Bas, Luuk, Ralph and my daily supervisor Guangze. Without your patient guide and support, I can never complete my thesis work successfully. Secondly, I want to show my gratitude to my sincere friends Yidan, Sihan, Haozheng, Qianxue, Yuhao, Yiqian, Tianyi, Connie. You guys made my life in TUD colorful and enjoyable. Especially Yidan and Sihan who constantly support me during tough times and helped me with my accommodation, I can never show enough gratitude to you two wonderful homies. Finally, I want to say thank you to my parents who always give me their love and support.

The life in Delft is my treasure and I will never forget my experience in Delft.

Hao Liu

August 2022

Content

1. Introduction

1.1 Research background

Oil-in-water waste streams can be produced by steel, food and other industries and has become a severe water pollutant in recent years. Treatment methods are usually costly and ineffective (Abadi, Sebzari, Hemati, Rekabdar, & Mohammadi, 2011; Cui, Zhang, Liu, Liu, & Yeung, 2008). Traditional treatment methods of oily wastewater include gravity settling followed by skimming, dissolved air flotation, coagulation and flocculation, and chemical de-emulsification (Cheryan & Rajagopalan, 1998). With the development of water treatment technology in the past decades, membrane separation has been increasingly used for oil/water emulsion treatment and proved to be an effective and efficient method in treating the oily wastewater (Cui et al., 2008). Among all types of membranes, the ceramic membrane has the following advantages in treating oily wastewater: 1) no chemical addition during treatment, 2) higher fluxes which results from its high porosity and hydrophilicity, 3) chemical stability (Abadi et al., 2011; Chen et al., 2021; Motta Cabrera, Winnubst, Richter, Voigt, & Nijmeijer, 2021). However, membrane fouling is unavoidable in membrane separation and serves as a major reason for a decrease in permeate flux, a larger transmembrane pressure (TMP), as well as more energy consumption (M. Chen et al., 2021).

1.2 Knowledge gap and research objectives

Oil-in-water emulsions have oil droplets with size ranging from tens of nanometers to hundreds of micrometers. The treatment of micron-sized O/W emulsions has been investigated in several studies using different types of membranes such as siliciumcarbide, alumina, and zirconia membranes (M. Chen, Heijman, Luiten-Olieman, & Rietveld, 2022; Y. Chen & Liu, 2020; Cheryan & Rajagopalan, 1998; N. Gao & Xu, 2019; Qin, 2021). Nano-sized O/W emulsions are more difficult than micron-sized O/W emulsions to treat because of their small sized droplets, and there

are studies dealing with the separation of nano-sized O/W emulsions using zirconia, polymeric, and cellulose membranes (M.-X. Hu, Niu, Chen, & Zhan, 2019; D. Li et al., 2019; Wang et al., 2022). However, studies on the filtration of nano-sized O/W emulsions using alumina membranes have not been reported yet. Hu et al (2019) found that membranes with mean pore size of 312 nm could achieve an oil rejection over 99% even the size of oil droplets were smaller than 60 nm. This phenomenon has also been found in other studies and the mechanism was not well understood (Hu et al., 2019; Wang et al., 2022). Possible explanation was that a cake layer was formed on the membrane wall during the separation progress and thereby sieving the smaller sized oil droplets (Wang et al., 2022). This thesis aimed to find out the influence of membrane pore size on oil rejection and fouling of alumina membranes when treating the nano-sized oily wastewater and then find out the largest acceptable pore size of alumina membranes to treat the nano-sized O/W emulsions. Therefore, the objective of this study is to investigate the influence of membrane pore size, pH, salinity, and cross flow velocity on the rejection of nano-sized oil droplets as well as the fouling in the membrane separation of nano-sized O/W emulsions.

1.3 Research questions and approaches

Based on the knowledge gap and research objectives, this thesis aims to find out the answers to the following four research questions:

1) What is the influence of different cross flow velocities on membrane fouling?

2) What is the influence of the membrane pore size (100, 200, 400, 600, 800 nm) on membrane fouling and oil rejection?

3) What is the influence of pH on membrane fouling?

4) What is the influence of salinity on membrane fouling?

And the hypotheses to the research questions is:

1) With higher cross flow velocities, the membrane fouling will be less due to the high turbulence.

2) With larger pore size, the oil rejection will be lower and there will be less fouling.

3) With higher pH, there will be less fouling.

4) With higher salinity, there will be more fouling.

To answer the above research questions and verify the hypotheses, literature review and laboratory experiments were done to obtain results and draw conclusions. The thesis is structured in the following way.

Chapter 1 gives the general background information of this study and provides the relevant research questions.

Chapter 2 describes previous studies including the preparation of the alumina membrane, nano-sized O/W emulsions and demonstrations of main fouling mechanism of alumina ceramic membrane. When the research started, the collected experimental data were analyzed and explained based on the literature to ensure the theoretical accuracy of the results.

To answer the research questions, laboratory experiments such as infiltration test was conducted to collect the transmembrane pressure with filtering time and frequency. Chapter 3 presents the details of the experiment set-up and procedure.

Chapter 4 plots, illustrates, and discusses the results of the experiments.

Chapter 5 answers the research questions and concludes the main findings of the study.

Chapter 6 demonstrates the limitations of current study and provides suggestions for future study and application.

2. Literature review

2.1 Alumina membranes in water treatment

During the membrane filtration process, substances such as suspended solids and colloids in the feed stream can be retained in the concentrate, and pure water can be collected as permeate which is produced in the filtration process driven by TMP. Membrane separation has been increasingly popular in oily wastewater treatment due to its high oil rejection ratio, high efficiency, and low operation cost (Bayat, Mahdavi, Kazemimoghaddam, & Mohammadi, 2016; M. Chen et al., 2022; Cui et al., 2008; Yang, Zhang, Xu, & Shi, 1998).

Among different types of membranes, ceramic membranes have been proven to be a promising method to filtrate O/W emulsions due to its chemical stability, high flux, and easy cleaning (Abadi et al., 2011; M. Chen et al., 2021; Motta Cabrera et al., 2021). Alumina, zirconia, titania, and silica are most commonly used material for manufacturing ceramic membranes (Amin, Abdallah, Roushdy, & El-Sherbiny, 2016; Cui et al., 2008; Yang et al., 1998). Among the above ceramic membranes, alumina membranes is the most widely used membranes (Yang et al., 1998). The characteristics of alumina membranes are further illustrated in the sections 2.1.1 and 2.1.2.

2.1.1 Zeta potential of alumina membranes

Zeta potential can show the surface charge of membranes and is an electrical potential which plays a vital role in the interactions between particles and particles, or particles and surfaces (Huisman, Trägårdh, Trägårdh, & Pihlajamäki, 1998). As zeta potential is an important measure of the surface charge of the membranes, it is an important parameter affecting the fouling and oil rejection in membrane separation. Therefore, it is important to know the zeta potential of alumina membranes used in the filtration

process.

According to previous studies, zeta potential of alumina membranes is mainly affected by pH (M. Chen et al., 2022; de Lint et al., 2003; Huisman et al., 1998; Nagasawa, Omura, Asai, Kanezashi, & Tsuru, 2020). It has been demonstrated that zeta potential of many membranes, including alumina membrane, has a positive value at low pH and a negative value at high pH, and the point where the zeta potential turns from positive to negative is named the “iso-electric point” (M. Chen et al., 2022; de Lint et al., 2003; Huisman et al., 1998). Figure 1 shows the changing zeta potential of α-alumina with the pH measured in two studies (M. Chen et al., 2022; Nagasawa et al., 2020). In this study, the feed stream was around 5.8. And according to Figure 1, the alumina membranes have a negative value at pH 5.8.

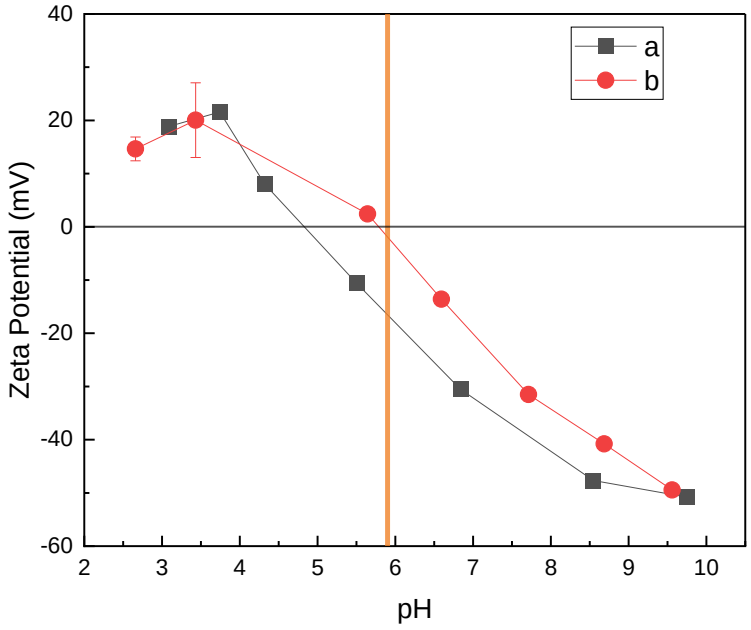

Figure 1. Zeta potential measurement for alumina membranes. Line a was adapted from the measurement by Nagasawa et al. (2020) and line b was adapted from the measurement by M. Chen et al. (2022). The orange line represents the pH value of the feed stream used in filtration experiments which is around 5.8.

2.1.2 Chemical and thermal stability of alumina membranes

Van Gestel et al. (2002) explored the chemical stability of alumina membranes and the results showed that when under acidic condition, alumina membranes showed a high corrosion resistance when pH was higher than 3, and an even better corrosion resistance in strong acid if the membrane was previously treated under high temperature (1000 ˚C). When under alkaline condition, alumina membranes showed a high corrosion resistance up to pH 11 (Van Gestel et al., 2002). Therefore, it can be concluded that alumina membranes have a high chemical stability when pH ranges from 3 to 11. Therefore, it is feasible to clean the alumina membranes using sodium hydroxide solutions or citric acid solutions.

Apart from the chemical stability, studies have shown that alumina membranes were stable after treatment with high temperature up to 700 ˚C (Chang, Gopalan, & Lin, 1994). Therefore, it is also feasible to clean the alumina membranes using thermal treatment (200 ˚C).

2.2 Fouling in membrane separation

2.2.1 Fouling mechanisms in separation of O/W emulsion

In spite of all these advantages which ceramic membranes have, membrane fouling is still an inevitable problem which occurs during the separation process. Membrane fouling can lead to more energy consumption, shorter membrane life, more cleaning cost, and lower separation efficiency compared to unfouled membranes. Therefore, it is important to know the mechanism and solve the fouling problem.

Depending on whether the fouling can be removed by certain cleaning methods, membrane fouling can be divided into reversible fouling and irreversible fouling (Shi, Tal, Hankins, & Gitis, 2014; Yamamura, Kimura, & Watanabe, 2007). After a certain cleaning method such as backwash, reversible fouling can be removed and

irreversible fouling cannot be removed (Shi et al., 2014). The cleaning methods includes hydraulic approach like backwash, and chemical approach like acid or alkaline cleaning. The review of the cleaning methods can be found in section 2.4.

According to Hermia's theory, the fouling mechanisms in membrane separation can be generally summarized as the following different forms: 1) complete pore blocking; 2) standard pore blocking; 3) intermediate pore blocking; and 4) cake filtration (Hermia, 1982b). Based on Hermia's equations for constant pressure filtration experiments, several authors have developed different combined models to explain the fouling in different filtration experiments under different conditions (Bolton, LaCasse, & Kuriyel, 2006; Bowen, Calvo, & Hernández, 1995; Field & Wu, 2011; Ho & Zydney, 2000).

The schematic illustration of the above four fouling mechanisms is shown in Figure 1 (Kirschner, Cheng, Paul, Field, & Freeman, 2019).

The phenomenon in which the membrane pores are fully or partially clogged by particles or colloids is named pore blocking (Field & Wu, 2011). It typically occurs quickly in the early phases of membrane separation because at that time the membrane surface is free of deposits and the entering particles and colloids can directly connect with the membrane pores (Shi et al., 2014).

Complete pore blocking occurs when foulant colloids which have identical size with the membrane pores deposit onto the open surfaces and totally obstruct the pores in the covered area (Hermia, 1982b).

Comparable to complete pore blocking, intermediate pore blocking allows for the deposition of particles on top of one another. The foulant colloids can possibly deposit on the uncovered membrane surface or the colloids that already block the membrane pores (Kirschner et al., 2019).

Different from complete and intermediate pore blocking, standard pore blocking takes place inside the membrane pores. When the particles or colloids have a smaller size than the membrane pores or can be deformed during the filtration process, they can deposit inside the membrane pores and thereby cause blockage (Hermia, 1982b).

Cake filtration refers to the process where particles or colloids accumulate on a membrane's surface layer by layer, which is known as the fouling cake formation, resulting in an increase in the energy consumption to produce the permeate flow (Shi et al., 2014). The cake layer formed on the membrane surface in the early stage of the membrane separation can inhibit direct interaction between further foulants and the membrane surface. A previous study has shown that using cellulose membrane which has a pore size of about 312nm to filtrate oil in water nano emulsions with size ranged from 6 to 60 nm, the oil rejection is higher than 99% (M.-X. Hu et al., 2019). Wang et al. (2022) also found the same phenomenon and they explained the unexpected high oil rejection by using the cake filtration mechanism that a cake layer is formed by the deposited large oil droplets at the starting phase of the separation process and the cake layer then blocks oil droplets with size smaller than membrane pore size (Wang et al., 2022).

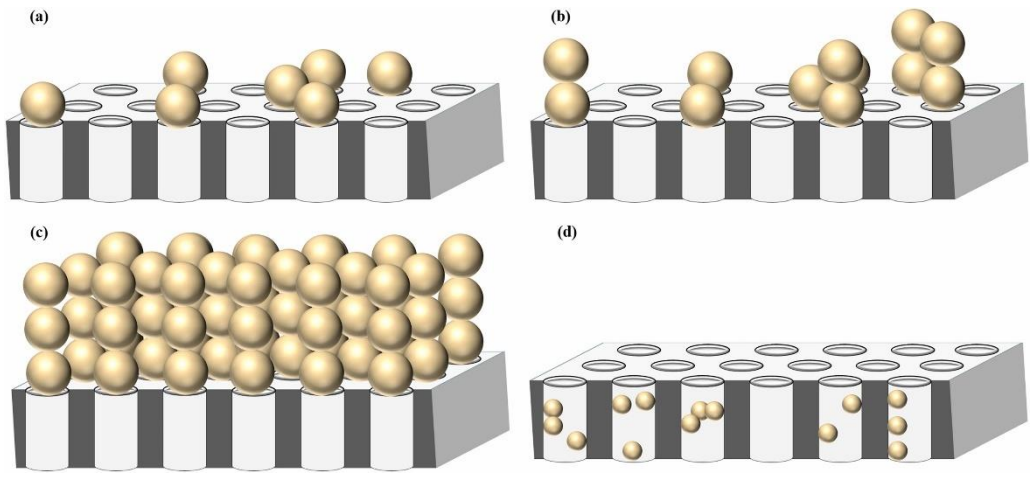

Figure 2. “Schematic illustration of Hermia’s four fouling mechanisms: (a) Complete

pore blocking, (b) Intermediate pore blocking, (c) Cake filtration and (d) Standard pore blocking" (Kirschner et al., 2019).

Despite all these studies on the fouling mechanisms of membrane filtration, the fouling mechanism of UF membrane separation of O/W emulsions has not been well understood. In most cases, the fouling is caused by a combination of different kinds of fouling mechanisms making it more difficult to investigate. In this thesis, a qualitative test was done in the filtration experiments to investigate the influence of different membrane pore sizes to find out the reason why membrane with pore size larger than oil droplets can have high oil rejection.

2.2.2 Influential factors in crossflow filtration

The factors that can affect the fouling in membrane separation include: 1) characteristics of feed stream, 2) characteristics of membrane, 3) different operation conditions (Shi et al., 2014; C. Y. Tang, Chong, & Fane, 2011).

The pH value and ionic strength are the representative feed stream properties that can have an impact on the fouling during ultrafiltration. Previous studies have shown that with the increase in wastewater pH value, the fouling resistance also increased which resulted in less fouling (Contreras, Kim, & Li, 2009; B. Z. Dong, Chen, Gao, & Fan, 2006; Yuan & Zydney, 2000). One explanation to the effect of pH on membrane fouling was based on the Derjaguin–Landau–Verwey–Overbeek (DLVO) theory. DLVO theory indicates that the electrical interactions and the van der Waals forces are two dominant factors for the determination of the stability of colloids (Ohshima, 2012).The increased pH can promote the deprotonation of acidic functional groups in macromolecules such as protein and humic acids, which leads to the increase in the electrostatic repulsion between these molecules, inhibiting the build-up of cake/gel layer and increase the fouling resistance (Contreras et al., 2009; Jones & O'Melia, 2000). Apart from its influence on the foulant in the wastewater, pH can also change the fouling resistance by affecting the surface charge of the membranes. The

relationship between the zeta potential of alumina membranes and pH values are shown in Figure 1. It is clearly shown that within the pH range from 4 to 10, the zeta potential of the alumina membranes became more and more negative. For the nano-sized O/W emulsions, the zeta potential of the colloidal foulants depends on the charge of the surfactant used. In this study, all the surfactants used were negatively charged. Therefore, it can be predicted that the higher pH will promote the electric repulsion between the membrane surface and the oil droplets and results in less fouling.

High ionic strength can also make the fouling more severe during the filtration of colloidal foulants. The electrical double layer (EDL) of oppositely charged ions is compressed with an increased ionic strength, which lead to a decreased electric repulsive energy barrier between molecules, allowing the van der Waals forces between molecules to take control (K. L. Chen, Mylon, & Elimelech, 2006). This leads to colloidal instability, which intensifies aggregation and results in higher fouling cakes (K. L. Chen et al., 2006; S.-z. Li & Xu, 2008; Sprycha, 1989). As mentioned above, with the addition of surfactants, the nano-sized O/W emulsions in this study were negatively charged. However, with the increase in ionic strength, the zeta potential of the nano-sized wastewater will become more positive because of the compression of the EDL, which decreases the electrical repulsion between the oil droplets and the membrane surface and results in more severe fouling.

The characteristics of membranes that can affect the fouling include membrane pore size, surface charge and density, and surface hydrophilicity. In this study, the focus was on the membrane pore size and the surface charge.

Several studies investigated the relationship between membrane pore size and membrane fouling using the fouling models (Hwang, Liao, & Tung, 2008; Kirschner et al., 2019). The derived membrane fouling model under constant pressure (Hermia, 1982a) is shown in equation 1:

$$\frac{d^2t}{dv^2} = K(\frac{dt}{dv})^i \quad (1)$$

Where:

t is filtration time,

v is the received filtrate volume per unit filtration area,

i is the blocking index,

K is the resistance coefficient.

The blocking index i indicates the fouling mechanisms and is shown in Table 1.

Table 1. Index i and corresponding fouling mechanisms (Hwang et al., 2008)

Index i	Fouling mechanism
2	Complete blocking
1.5	Standard blocking
1	Intermediate blocking
0	Cake filtration

So far as we concerned, previous studies only investigated the relationship between membrane pore sizes and fouling when the membranes had a pore size smaller than the foulant's size (Hwang et al., 2008; Wang et al., 2022). This is because the membrane filtration of O/W emulsions has been assumed to be based on the physical separation, therefore, to obtain an ideal oil rejection, smaller sized membranes are required. In the study of Wang et al. (2022), a summary of the previous work on the membrane separation of O/W emulsions listed their water permeance, oil droplet size and oil rejection. The summary is shown in Table 2.

Table 2. Comparison of membrane pore size, oil droplet size and oil rejection between different ceramic membranes reported in previous studies (Wang et al., 2022).

Membrane	Pore size (μm)	Oil droplet size (μm)	Oil rejection (%)	references
ZrO_2-Al_2O_3	0.85	1	99.8	(Yang et al., 1998)
TiO_2-Mullite	0.11	1.09	97	(Zhu et al., 2019)
Al_2O_3	0.4	1	82.7	(N. Gao & Xu, 2019)
Al_2O_3	0.35	1.43	99.6	(Zhong, Xing, & Zhang, 2013)
Mullite	0.19	1	>97	(Liu et al., 2020)
Kaolin	0.2	5	98.5	(Zou et al., 2021)
SiC	0.4	1	98.5	(Jiang et al., 2020)
Al_2O_3	0.2	2	>97	(H. Tang et al., 2018)
SiOC	0.95	0.83	94.6	(B.-B. Dong et al., 2019)
Zirconia	78nm	18nm	>99.7	(Wang et al., 2022)

Despite several studies have been working on the effects of membrane pore size on the fouling, the exact mechanisms were not well understood. In some works, with the increase in the membrane pore sizes, the fouling became more severe. The proposed explanations include: 1) when membrane pore sizes become larger, more oil droplets can get into the membrane pore and result in more pore blocking (Hwang et al., 2008); 2) the higher surface roughness as a result of the larger membrane pore sizes can lead to stronger interactions between oil droplets and membrane surface and thereby result in more severe fouling (Wang et al., 2022). Apart from the negatively

related pore size and membrane fouling found in these studies, some studies found that larger membrane pore sizes could result in less fouling. The explanation to this phenomenon is based on the hydrophilicity of the membrane materials. It was suggested to study the influence of membrane pore size together with the membrane material's hydrophilicity. For polyvinyl fluoride (PVDF) membranes, which is a hydrophobic material, the larger the membrane pore size is, the less fouling will be occurred (Miyoshi et al., 2015).

The surface charge of alumina membranes is positive at low pH and negative at high pH which can be seen from Figure 1. Therefore, when the nano-sized O/W emulsions are added with anionic surfactants like SDS, it is supposed that less fouling will result from a higher pH because it will encourage the electrostatic repulsion between the membrane surface and the oil droplets.

Operation conditions generally refer to the hydrodynamic factors which can be changed during the membrane filtration process. It is universally acknowledged that operation conditions have significant influence on the fouling in membrane separation by utilizing the fluid behaviors, and the conditions include parameters such as cross flow velocity and feed flux (Goosen et al., 2005; Jung & Ahn, 2019). cross flow velocities can affect the fouling by changing the shear force on the membrane wall during the separation process and thereby influencing the deposition of the foulant onto the membrane wall (Kirschner et al., 2019). Reynolds number (Re) is the indicator to show the fluid flow patterns. When Reynolds number is low, the flow is called laminar flow. When Reynolds number is high, the fluid will consist of eddies and is named turbulent flow. The general definition of Re of the fluid in a tube is shown in the following equation (Munson, Okiishi, Huebsch, & Rothmayer, 2013):

$$Re = \frac{\rho u d}{\mu} \tag{2}$$

Where:

P is the fluid density,

u is the fluid mean velocity,

d is the hydraulic diameter of the tube,

μ is the dynamic viscosity of the fluid.

As we can see from the equation, a higher cross flow velocities leads to a higher Reynolds number which indicates a more turbulent flow. Studies has shown that particle deposition decreases with the increasing cross flow velocities as the flow becomes more turbulent when the cross flow velocities increases, which means that the shear stress near the membrane wall dominates the flow pattern and removes the particles or colloids that deposited previously (Jung & Ahn, 2019). Therefore, it is concluded that a higher cross flow velocities will lead to less cake layer formation and thereby reduce membrane fouling.

It is universally acknowledged that higher flux will result in more severe fouling. The concept of threshold flux is proposed to distinguish the low fouling and the high fouling region. By definition, “the threshold flux is that flux at or below which a low and near constant rate of fouling occurs but above which the rate of fouling increases markedly” (Field & Pearce, 2011).

2.3 Nano-sized O/W emulsion

Oil plays an important role in modern civilization and can be used in many ways in people’s life. However, the wastewater containing oil can be produced from many industries like petroleum refining, pharmaceutical manufacture, and food industries (Y.-M. Lin & Rutledge, 2018). The oily wastewater can cause damage to environment and public health due to its large quantity, consumption of dissolved oxygen and potential impact on human health (M. Chen et al., 2022; Y. M. Lin, Song, & Rutledge, 2019). Based on the size of oil droplets, the oil in the wastewater can be divided into three forms: free, dispersed, and emulsified. The O/W emulsions are characterized by the oil droplets with the size smaller than 20mm (Y.-M. Lin &

Rutledge, 2018; Rhee, Martyn, & Kremer, 1987). In emulsified oily wastewater, nano-sized oil droplets which have the size below 200nm are commonly found and their small size makes them much more difficult to be removed from the stream (Fakhru'l-Razi et al., 2009; L. Hu et al., 2015). Generally, the emulsified oil droplets have high colloidal stability due to the use of surfactant and have a long settling time (Kajitvichyanukul, Hung, & Wang, 2011). Therefore, the conventional method to remove the nano-sized oil droplets consists of de-emulsification with the addition of chemicals and followed with the separation by gravity (Križan Milić, Murić, Petrinić, & Simonič, 2013).

Soybean oil is abundantly used in food industries and making it a commonly seen foulant in wastewater (Hammond, Johnson, Su, Wang, & White, 2005). Therefore, soybean oil was used for synthesizing of nano-sized O/W emulsions in this thesis as it has been proved to be able to form nano-sized oil droplets in previous study (Wang et al., 2022). The physical properties are summarized in Table 3. Soybean oil can react with oxygen and high temperature can accelerate the reaction process (Hammond et al., 2005), so the processing and storage of the soybean oil are kept at low temperature to avoid the change of quality of the soybean oil. Besides, soybean oil droplets are a deformable foulant and can form both cake layer and pore blocking during the filtration process. The method of synthesis of the nano-sized O/W emulsions will be introduced in chapter 3.

Table 3. Physical properties of soybean oil concluded by Hammond et al. (2005).

Properties	
Density at 20 ˚C	0.9165 - 0.9261 g/ml
Specific heat capacity at 20 ˚C	0.448 cal/(g ˚C)
Surface tension at 20 ˚C	26.8 dyne/cm
Viscosity at 20 ˚C	58.5–62.2 cP

Melting point	0.6 ˚C

2.4 Membrane cleaning

Because of the fouling happening during the filtration process, the permeance of the membrane may decrease and cause an increase in the energy consumption or a decrease in the permeate flux. Membrane cleaning aims to recover the separation performances of the membrane (Blanpain-Avet, Migdal, & Bénézech, 2009). The cleaning methods are divided into physical cleaning and chemical cleaning based on whether there is addition of chemical agents (Shi et al., 2014).

2.4.1 Physical cleaning

Physical cleaning can remove the particles or colloids attached to the surface wall of the membrane by using the mechanical forces like shear stress and pressure difference (Trägårdh, 1989). There are many techniques in physical cleaning, and in this thesis, the used techniques are backwash and forward flush which are the most common methods to clean the fouled membranes. The schematic illustration of the two processing methods is shown in Figure 3 (Blandin, Verliefde, Comas, Rodriguez-Roda, & Le-Clech, 2016).

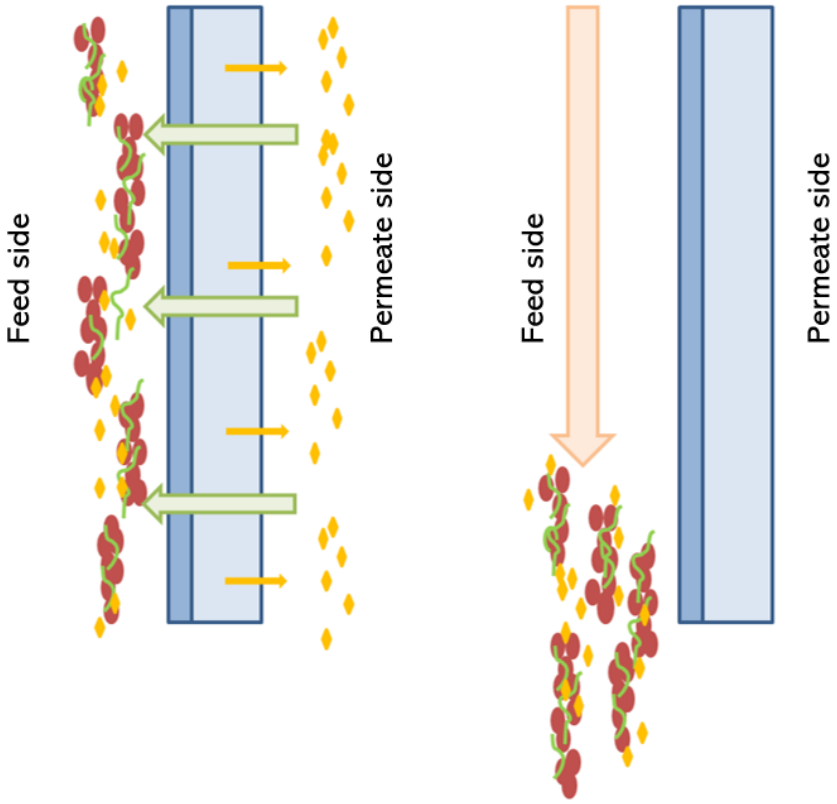

Figure 3. Schematic illustration of backwash (left) and forward flush (right) cleaning methods (Blandin et al., 2016)

To recover the hydraulic reversible fouling, the membrane is backwashed by a reversed flow driven by the pressure difference and pushed from the permeate side to the feed side of the membrane (W. Gao et al., 2011). On the membrane surface, the formed cake layers during the separation process are loosened and the deposited foulants on the pores are dislodged by the reversed flow (Shi et al., 2014). The required flux for backwashing is typically two times higher than the permeate flux. Because of the high flux and high pressure performed during the backwash process, the membrane could be damaged. Ceramic ultrafiltration membranes can withstand the backwash flow and therefore backwash can be used to clean the alumina ultrafiltration membranes used in this study (Baker, 2012).

Forward flush refers to the cleaning process where the particles deposited on the

membrane surface are removed by a turbulent cross flow with high velocity (Verberk & van Dijk, 2003). The operation of the forward flush is similar to the membrane filtration process instead that the feed stream is changed to the cleaning stream and the cross flow velocities is increased.

2.4.2 Chemical cleaning

By addition of different kinds of chemical agents, chemical cleaning aims to remove the hydraulically irreversible fouling that cannot be removed by physical cleaning. A previous study has shown that cleaning the membrane in 0.01M NaOH solution with water bath of 65 ˚C for 1 to 2 hours can effectively remove the hydraulically irreversible fouling (Chen et al., 2022).

3. Materials and Methods

3.1 preparation of ceramic membrane

Alumina ultrafiltration membranes (coorsTek, the Netherlands; Inopor GmbH, Germany) with different pore sizes (100nm, 200nm, 400nm, 600nm, 800nm) were used to separate the nano-sized oil droplets from water in the O/W emulsions. The properties of the alumina UF membranes are summarized in Table 4.

Table 4. Properties of alumina UF membranes used in this experiment.

Properties	unit	coorsTek	Inopor GmbH
Pore size	nm	100	200, 400, 600, 800
Clean water permeance	$bar^{-1}L\ m^{-2}\ h^{-1}$	385	1200, 3000, 3700, 5000
Length	cm	10	10
Sealed length	cm	2	2.6
Inner diameter	mm	6	7
Outer diameter	mm	10	10
Filtering area	m^2	0.001508	0.001627

For membranes with 100nm pore size (coorsTek, the Netherlands), the inner diameter and outer diameter were 6 mm and 10 mm, respectively. The length of the membrane was 10 cm, and the membrane was sealed manually on both ends and the total length of the sealed area was 2 cm. Therefore, the effective filtering area of the membrane was calculated to be 0.001508 m^2. For membranes with a pore size of 200nm, 400nm, 600nm, and 800 nm (Inopor GmbH, Germany), the inner diameter and outer diameter

were 7 mm and 10 mm, respectively. The length of the membrane was 10 cm, and the producer sealed the membranes on both ends of the membranes with glass and the total length of the sealed area is 2.6 cm. Therefore, the effective filtering area of the membrane was calculated to be 0.001627 m^2. Based on a preliminary experiment, the average permeance of the membrane with pore size of 100 nm was 385 ± 30 L m^{-2} h^{-1} bar^{-1}, and the average permeance of the membrane with pore size of 200, 400, 600, 800 nm was 1200±100 L m^{-2} h^{-1} bar^{-1}, 3000±200 L m^{-2} h^{-1} bar^{-1}, 3700±200 L m^{-2} h^{-1} bar^{-1}, and 5000±300 L m^{-2} h^{-1} bar^{-1}, respectively. The two different kinds of alumina membranes are shown in Figure 4.

Figure 4. Photos of alumina membranes from coorsTek (left) and Inopor GmbH (right)

3.2 synthetization of nano-sized O/W emulsions

In this research, nano-sized O/W emulsions with a concentration of 500 mg/L were synthesized and stabilized by the addition of mixed surfactant Span 80 and Tween 80 with the mass ratio of approximately 1:1(Wang et al., 2022). The critical micelle concentration (CMC) for Span 80 in paraffin oil is 184.3 mg/L, and the CMC for Tween 80 in oil is 2500 mg/L (Schmitt, Limage, Denoyel, & Antoni, 2016; Bide, Fashapoyeh, & Shokrollahzadeh, 2021). Therefore, to effectively stabilize the nano-

sized O/W emulsions, the Tween 80 and Span 80 concentration was obtained at 50 mg/L for the synthetization of 500mg/L nano-sized O/W emulsions, therefore the mass ratio of oil, Span 80, Tween 80, and demineralized water was 0.5 : 0.05 : 0.05 : 1000 (Opawale & Burgess, 2011). The synthesis of nano-sized O/W emulsions was based on the following 2 steps:

1) Soybean oil (Signma-aldrich, Germany), Span 80, and Tween 80 (Signma-aldrich, Germany) were added into demineralized water (pH = 5.8) and then continuously stirred at 2000 rpm with a magnetic stirrer (L23, LABINCO, the Netherlands) for 24 hours.

2) Then the O/W emulsion was treated with ultrasonication in a sonifier (Branson Digital) for 24 hours until it appeared milky white (Wang et al., 2022; Yan et al., 2019; Zhan, Zuo, Tao, & Chang, 2018).

The emulsion remained stable and homogeneous for approximately three days. Before every experiment, a fresh emulsion was prepared using demineralized water with a constantly oil concentration (500 mg/L) since the typical value in oily wastewater ranging from 50 to 500 mg/L (Fakhru'l-Razi et al., 2009). Then, with the addition of NaCl, or HCl, or NaOH, or SDS, eight kinds of nano-sized O/W emulsions were produced for further filtration experiment and the composition of these eight kinds of nano-sized O/W emulsions are listed in the following Table 5.

The filtration experiments were designed to separate the oil droplets from the emulsion and are explained in detail in section 3.5. The comparison between filtering test with solution 2, 3 and 4 was to investigate the effect of salinity on the separation of O/W emulsion. The comparison between filtering test with solution 5, 6 and 7 was to investigate the effect of pH on the separation of O/W emulsion. Filtration tests with solution 1 were also used for determining the effect of pore size and cross flow velocity on the separation of O/W emulsion.

Table 5. Eight kinds of nano-sized O/W emulsions

Solution	Oil concentration (mg/L)	Tween 80 (mg/L)	Span 80 (mg/L)	SDS (mg/L)	NaCl (mmol/L)	pH
1	500	50	50	0	0	5.8
2	500	0	50	50	1	5.8
3	500	0	50	50	10	5.8
4	500	0	50	50	100	5.8
5	500	0	50	50	0	4
6	500	0	50	50	0	6
7	500	0	50	50	0	8
8	500	0	50	50	0	10

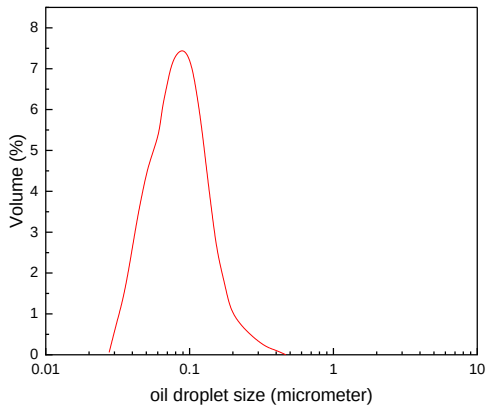

Figure 5. Particle sized distribution of oil droplets in nano-sized O/W emulsions

3.3 O/W emulsion characterization

In this study, nano-sized O/W emulsions were characterized by measuring its physical and chemical parameters including Chemical Oxygen Demand (COD), Particle Size Distribution (PSD), pH, and Zeta potential.

3.3.1 COD

A calibration curve of oil concentration versus COD was determined in advance and a linear relationship was found between oil concentration and COD. The oil concentration of nano-sized O/W emulsion in the study would then be determined based on the COD values measured with Hach-Lange Kits and the calibration curve measured in advance was shown in Figure 6.

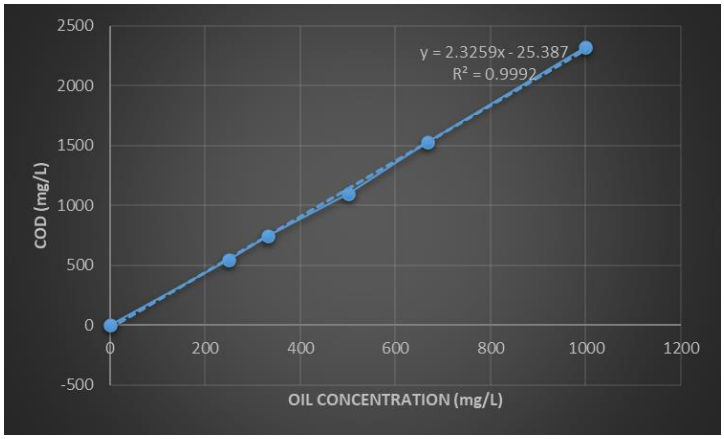

Figure 6. Calibration curve of oil concentration versus COD.

The oil rejection was calculated with equation 3.

$$R = \left(1 - \frac{F_p}{F_f}\right) \times 100\% \quad (2)$$

Where:

F_p was the oil concentration in the permeate,

F_f was the oil concentration in the feed stream.

3.3.2 PSD

The PSD of the oil droplet in the O/W emulsions was measured with a blue wave Microtrac SDC (Bluewave, Microtrac, USA). In this study, all the synthesized nano-sized O/W emulsions had an average particle size smaller than 200 nm.

3.3.2 Zeta potential

Zeta potential was measured to reflect the colloidal stability and charge of the nano-sized O/W emulsions. The zeta potential of feed stream samples was measured with the help from IHE Delft Institute for Water Education by a Malvern Zetasizer Nano ZS instrument (Zetasizer lab, Malvern, UK) and the results of the measurements were shown in section 4. Equation 4 shows the determination of zeta potential.

$$\zeta = \frac{4\pi\eta}{\varepsilon}\frac{v}{U/L} \quad (3)$$

Where:

η is the viscosity of water,

ε is the dielectric constant of water,

v is the mobile velocity of the oil droplets in the electric field,

U is the voltage,

L is the distance between the two electrodes.

3.3.3 pH

A pH sensor (inoLab™ Multi 3430 - WTW) was used to measure the pH of the nano-sized O/W emulsion.

3.4 Experimental Set-up

The fouling of the membrane and the oil rejection of the nano-sized O/W emulsions were determined with the constant flux experiments. The schematic set up for the

filtration experiments is shown in Figure 7. The system consists of a membrane module, a feed tank filled with O/W emulsion, a concentrate tank for the collection of concentrate after filtration, a backwash tank filled with demineralized water, a scale for the measurement of the permeate, a high-precision pressure transducers (GS4200-USB, ESI, UK) for the measurement of TMP, a cross flow meter and two pumps.

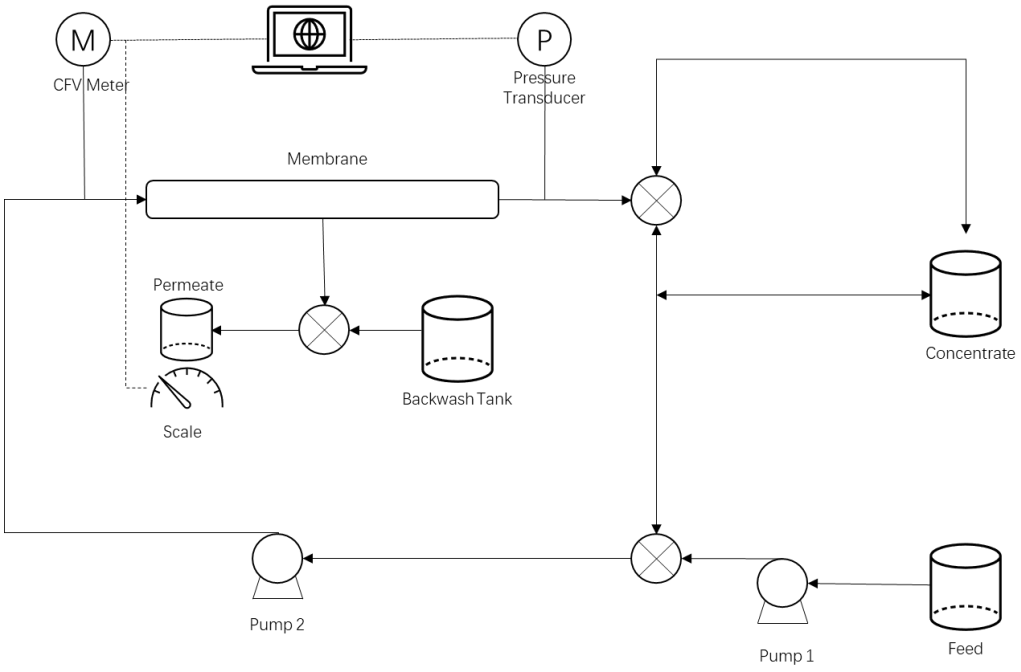

Figure 7. Experiment set up with constant flux

The feed stream was pumped into the system by pump 1 (Grundfos, DDA), which was used to control the influent flow rate. Given that the membrane was only 10 cm, the pressure difference between the two ends of the module can be ignored. The permeate flux pressure was zero. Therefore, the transmembrane pressure (TMP) could be measured using one high-precision pressure transducer (GS4200-USB, ESI, UK) at the location after the membrane module during the experiment. Pump 2 (Van Wijk & Boersma) was used to control the cross flow velocities and forward flush velocity.

3.5 Experimental procedure

First, a pure water filtration process to measure the permeance of the membrane was

conducted ahead of the filtration experiment. The permeance of the membrane was measured using demineralized water with a constant pressure system (3.2 bar) using the backwash tank. The permeance of the membrane was calculated using the equation 4.

Then before the filtration experiments started, the system was flushed with the feed stream to remove air bubbles in the pipes, the cross flow velocities for the forward flush was maintained at 2 m/s and the process lasted for 2 mins. After the air bubbles were fully exhausted, the filtration experiment was then conducted under a constant flow condition with different cross flow velocities s (0.35 m/s, 0.47 m/s, and 0.59 m/s) and membrane of different pore sizes (100nm, 200nm, 400nm, 600nm, 800nm).

Every filtration experiment had 4 to 6 cycles and each cycle lasted for approximately 22 mins. The permeate flux were measure and the membrane permeance was calculated every 30 seconds. For every cycle, there were three steps:

1) The first step was the filtration process. The duration of the filtration was typically 20mins and would be shortened when the fouling was too severe. The TMP during the filtration process was continuously monitored through computer, and once the TMP approached 1 bar, the filtration would be stopped to avoid too much fouling and keep the system safe. The filtration process was conducted under constant flux.

2) After the filtration process stopped, the hydraulic reversible fouling would be removed by backwash using the backwash tank under the pressure of 3.2 bar for 30 seconds.

3) Then before the next cycle started, the demi water was flushed out of the system by forward flush using feed stream for 15 s at a cross flow velocities of 2 m/s. After the forward flush, next cycle would start and follow the step 1 to 3.

When all the cycles were over, the filtration system were cleaned with forward flush for 5 minutes at a cross flow velocities of 2 m/s to drain the concentrate stream in the pipe to avoid fouling on the pipe wall. After that, the fouled membrane was taken out of the module and put into the bottle containing 0.01M NaOH solution for 2 hours at 65 ˚C water bath. In case the permeability of the membrane could not recover after chemical cleaning, thermal cleaning served as an alternative method to clean the membrane by putting the membranes in the oven under 200 ^{O}C for two hours. After chemical/thermal cleaning, the permeance of the alumina membrane was measured to make sure the membrane was fully cleaned. And filtration experiments of nano-sized O/W emulsions only started if the permeance of the membranes was recovered to more than 90% of the virgin membranes. All experiments were done in duplicate.

3.6 Data Analysis

The data analysis included the membrane permeance, TMP during the filtration process, the permeate flux, and the COD of the feed stream and permeate stream. The method of collecting these data was shown in section 3.3 and 3.5. Equation 4 was used to calculate the membrane permeance.

$$\mathrm{L} = \frac{\mathrm{J}}{\mathrm{TMP}} \tag{4}$$

Where:

L is the membrane permeance,

J is the permeate flux,

TMP is the transmembrane pressure.

Equation 5.1, 5.2, 5.3, 5.4 was used to calculate the reversible fouling resistance and irreversible fouling resistance.

$$J = \frac{\Delta P}{\mu(R_m + R_{rev} + R_{irrev})} \tag{5.1}$$

$$R_m = \frac{\Delta P_0}{\mu J} \quad (5.2)$$

$$R_{irrev} = \frac{\Delta P_b}{\mu J} - R_m \quad (5.3)$$

$$R_{rev} = \frac{\Delta P_e}{\mu J} - \frac{\Delta P_b}{\mu J} \quad (5.4)$$

Where:

J is the permeate flux,

ΔP is the transmembrane pressure,

ΔP_0 is the TMP of clean membrane at the start of the experiment,

ΔP_e is the TMP of membrane at the end of the experiment,

ΔP_b is the TMP of membrane after the backwash,

μ is the viscosity of the permeate stream,

Rm is the intrinsic membrane resistance,

Rr is the hydraulic reversible resistance,

Rirrev and hydraulic irreversible resistance

4. Results and Discussions

4.1 Effects of cross flow velocity on membrane fouling

The membranes used to investigate the effect of cross flow velocities on membrane fouling were all from coorsTek company with membrane pore size of 100nm. Using the step flux method (Beier & Jonsson, 2010; Choi & Dempsey, 2005; Le Clech, Jefferson, Chang, & Judd, 2003), when filtrating the 500 mg/L nano-sized O/W emulsions stabilized using surfactants Span 80 and Tween 80 at cross flow velocities of 0.59 m/s and 0.47 m/s, the threshold flux was determined to be 117 LMH and 88 LMH, respectively. The determination of the threshold flux is shown in Figure 8. Therefore, to have a clear view of fouling phenomena and ensure that the filtration experiment can last for 6 cycles, the flux was set to 100 LMH to investigate the effect of cross flow velocities on membrane fouling using constant flux experiments.

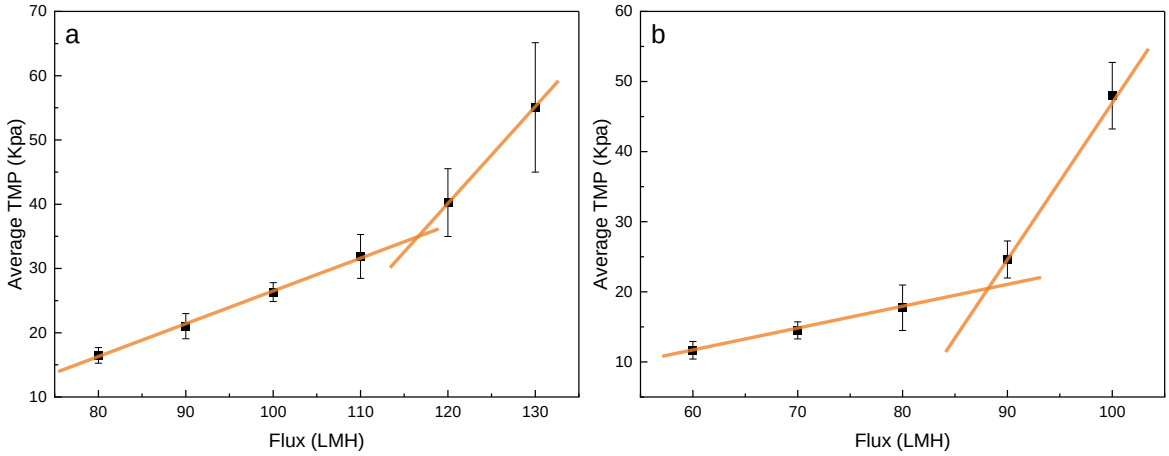

Figure 8. Threshold flux determination by step flux method for 100 nm alumina membranes filtering 500 mg/L nano-sized O/W emulsions stabilized using Span 80 and Tween 80 at cross flow velocities of (a) 0.59 m/s and (b) 0.47 m/s.

Apart from the cross flow velocities, the conditions of the filtration experiments are listed as follows: 1) pH = 5.8; 2) oil concentration = 500 mg/L; 3) temperature = 20 ±

3˚C; 4) feed flux = 100 LMH; 5) oil droplets mean size = 100 ± 10nm; 6) zeta potential of the feed stream = -21.3 ± 0.73 mV; 7) surfactant concentration = 50 mg/L Tween 80 + 50 mg/L Span 80. The results of the fouling are shown in Figure 9. It can be observed that with the increase in the cross flow velocities, the decline in normalized permeability became slower and the increase in normalized TMP became slower. This indicates that the increase in cross flow velocities was able to mitigate the membrane fouling. The explanation to this phenomenon was that with the increase in the cross flow velocities, the shear stress near the membrane wall became stronger and resulted in less deposition of oil droplets. The results are in accordance with the hypothesis and findings from previous studies (Jung & Ahn, 2019; Kirschner et al., 2019; Tanudjaja, Tarabara, Fane, & Chew, 2017).

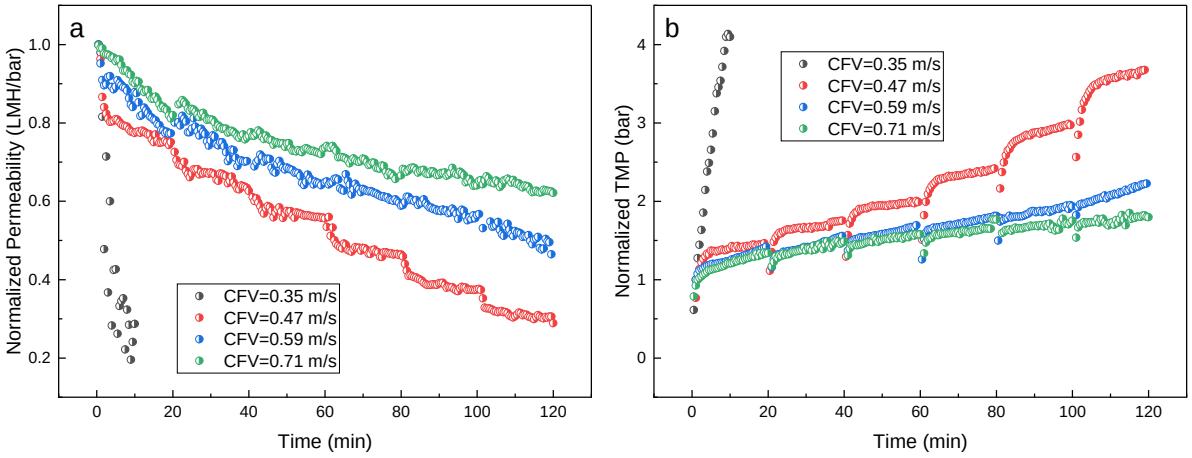

Figure 9. Normalized permeability (a) and TMP (b) curve for different cross flow velocities for 100 nm alumina membranes filtering 500 mg/L nano-sized O/W emulsions stabilized using Span 80 and Tween 80

The irreversible and reversible fouling resistance were calculated and shown in Figure 10. It was demonstrated that the irreversible fouling dominated the fouling for all the cross flow velocities experiments. Possible reason was that oil droplets which had sizes smaller than, equal to, or even slightly larger than the membrane pore size were squeezed into the membrane pores because of the deformability of the soybean oil

(Tummons, Tarabara, Chew, & Fane, 2016). Therefore, membrane pore blocking took control of the fouling and cake filtration only accounted for a small percentage. In all these experiments, the oil rejection was high (> 99.5%) which probably resulted from the cake layer formation and the structure of the membrane pore (Nagasawa et al., 2020; Wang et al., 2022).

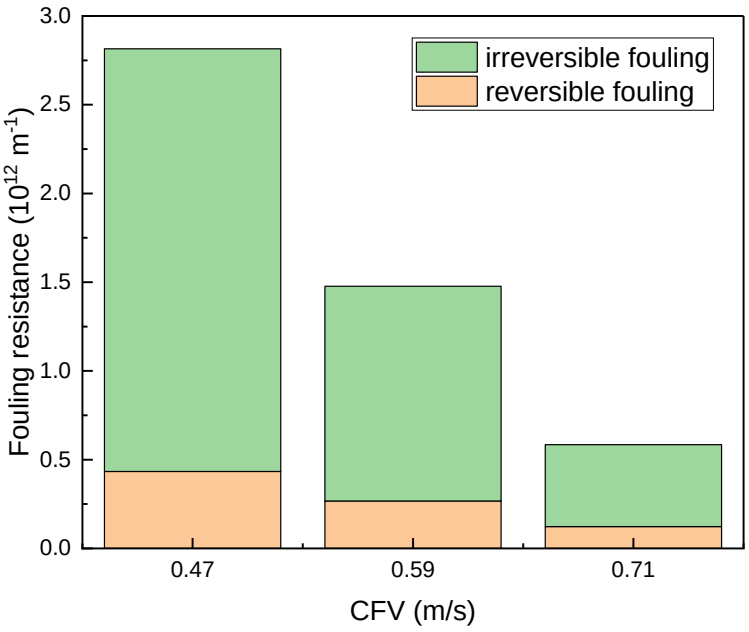

Figure 10. Irreversible and reversible fouling resistance for different cross flow velocities

4.2 Effects of membrane pore size

The membranes used to investigate the effect of membrane pore sizes on membrane fouling were all from coorsTek (100nm) and Inopor GmbH (200, 400, 600, 800 nm). Three different fluxes were applied for the study. The conditions of the filtration experiments are listed as follows: 1) pH = 5.8; 2) oil concentration = 500 mg/L; 3) temperature = 20 ± 3˚C; 4) feed flux = 40/ 60/ 100 LMH; 5) oil droplets mean size = 100 ± 10nm; 6) zeta potential of the feed stream = -21.3 ± 0.73 mV; 7) surfactant concentration = 50 mg/L Tween 80 + 50 mg/L Span 80.

4.2.1 Flux = 40 LMH

The results of the fouling and the oil rejection were shown in Figure 11. It can be observed that under the flux of 40 LMH, all these membranes were not fouled, probably because the flux is lower than the threshold flux of these membranes. Based on the PSD measurement of the feed stream, over 90% of the oil droplets had a size smaller than 200 nm. However, the oil rejection of the membrane with 200nm pore size was over 95%. The oil rejection decreased with the membrane pore sizes, and the membranes with pore sizes of 400, 600, and 800 nm also showed oil rejection. The explanation can be that during the filtration process, the oil droplets tended to deposit on the membrane wall and form a cake layer and reject the small-size droplets. Besides, the TMPs in these experiments were very low and probably failed to squeeze the oil droplets into the membrane pores (Tummons, Tarabara, Chew, & Fane, 2016). Also, some oil droplets could have been attached to the membrane wall because of the interaction between the membrane surface and oil droplets due to the roughness of the membrane surface (Wang et al., 2022; Kirschner et al., 2019). In addition, because the membrane pores were not uniform and the structure of the pores was not tubular, there could have been some narrow area which could be filled with oil droplets.

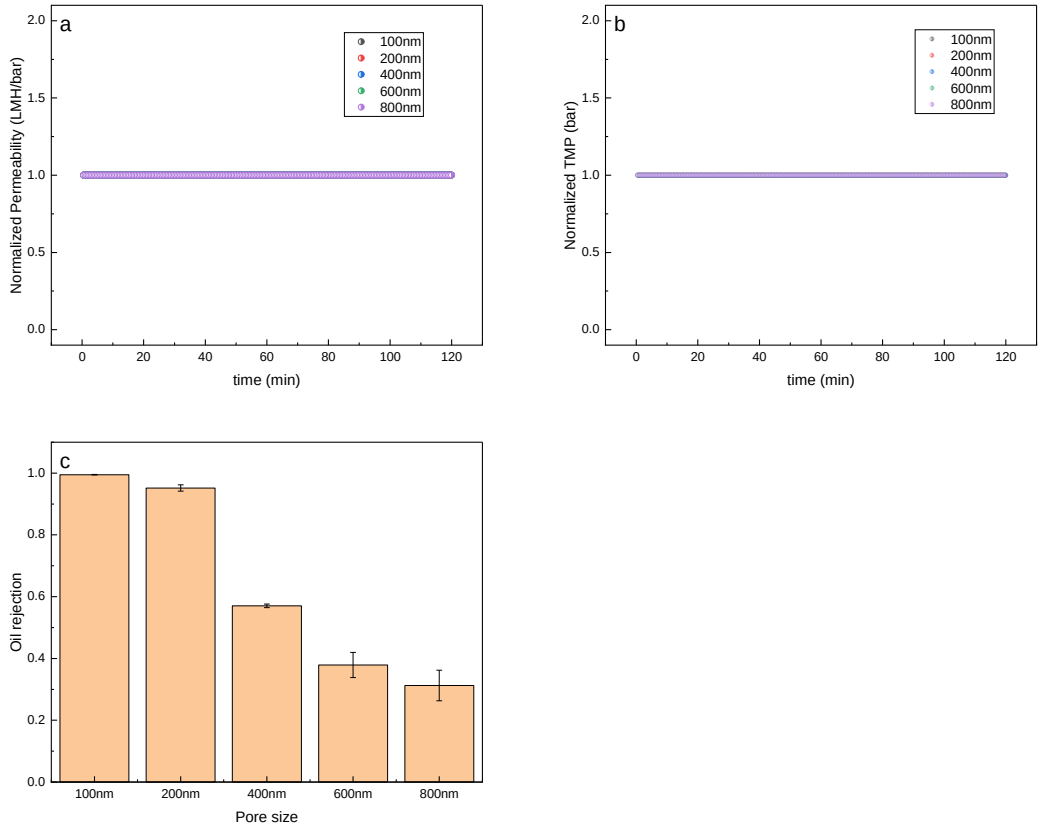

Figure 11. Normalized permeability curve (a), normalized TMP curve (b), and oil rejection (c) for alumina membranes with different membrane fore sizes filtering 500 mg/L nano-sized O/W emulsions stabilized using Span 80 and Tween 80 (flux = 40 LMH)

4.2.2 Flux = 60 LMH

The results of the fouling and the oil rejection are shown in Figure 12. It can be observed that when the flux increased to 60 LMH, membranes with pore size 200nm and 400nm were severely fouled, probably because that the flux was around the threshold flux of these membranes. The threshold flux of 800 nm and 600 nm membranes was larger than 60 LMH and therefore less fouling was observed in this membrane. Similar to the experiments when the flux was 40 LMH, the oil rejection of the membrane with 200nm pore size was over 95%. The oil rejection decreased with the membrane pore sizes, and the membranes with pore sizes of 400, 600, and 800 nm

still showed oil rejection.

To test the formation of a cake layer, the oil rejection was calculated from 0 to 2 min, 2 to 4 min, and 4 to 20 min in every cycle of the experiment with the 200 nm membranes. The results shown in Figure 12 (d) demonstrated that the oil rejection increased in the initial stage of the filtration process which verified the existence of cake layer formation. Besides, the large percentage of reversible fouling shown in Figure 13 also verified that the dominant fouling mechanisms was cake filtration.

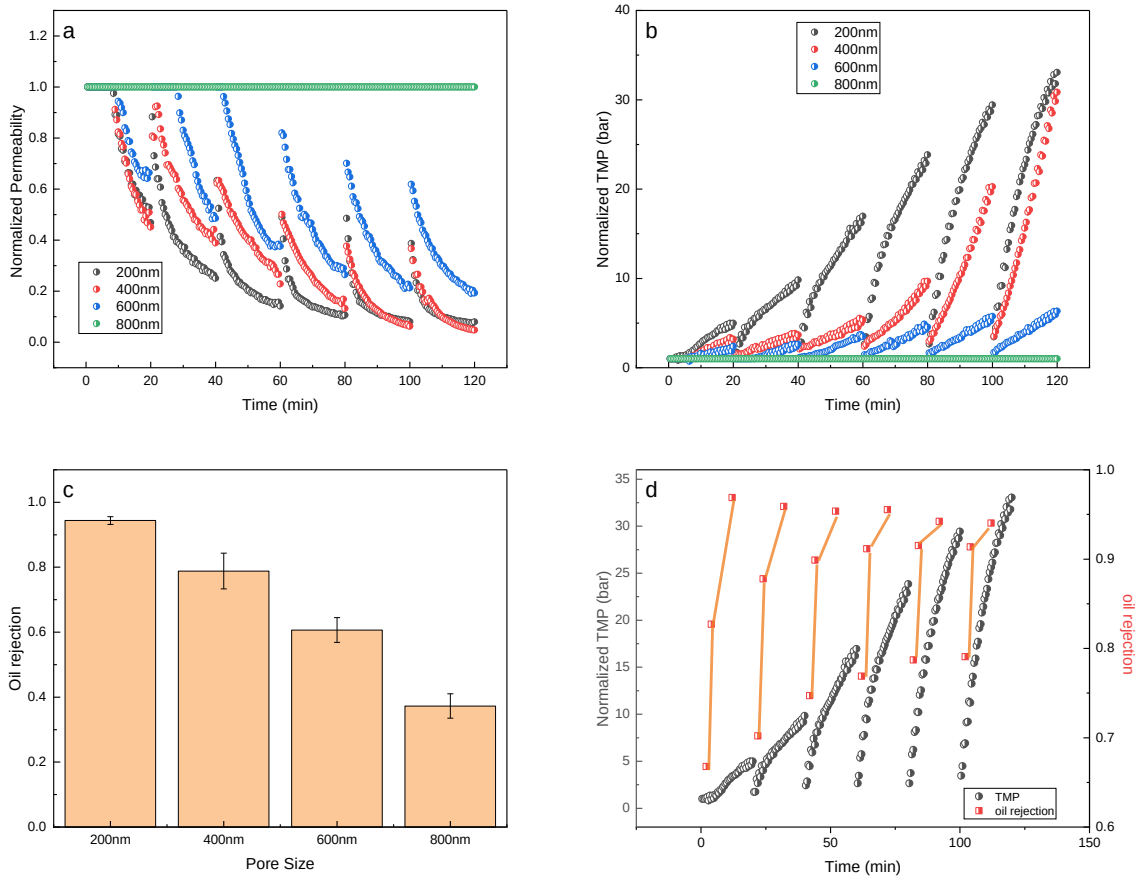

Figure 12. (a) Normalized permeability curve, (b) normalized TMP curve, (c) oil rejection for alumina membranes with different membrane fore sizes filtering 500 mg/L nano-sized O/W emulsions stabilized using Span 80 and Tween 80, (d) oil rejection and normalized TMP change with time for 200 nm membranes (flux = 60 LMH)

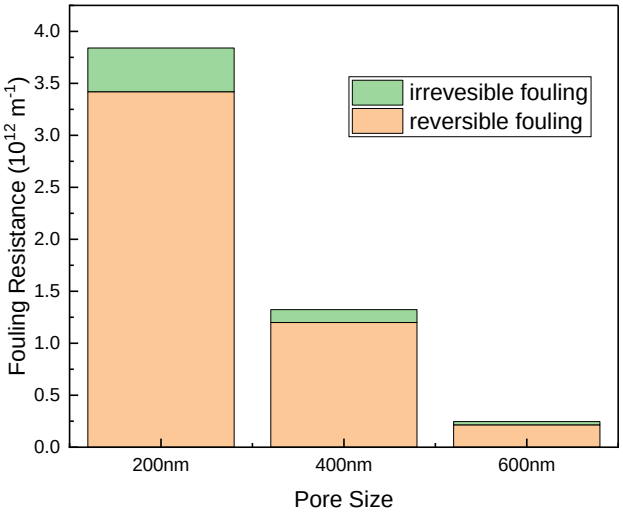

Figure 13. Irreversible and reversible fouling resistance for different membrane pore sizes

4.2.3 Flux = 100 LMH

The results of the fouling and the oil rejection were shown in Figure 14. It can be observed that when the flux increased to 100 LMH, the flux was beyond the threshold flux of the membranes with pore size 200 and 400 nm. The threshold flux of 600 nm was around 100 LMH and that of 800 nm was larger than 100 LMH. The oil rejection of the membrane with 200nm pore size was over 99%. The oil rejection decreased with the membrane pore sizes, while the membranes with pore sizes of 400, 600, and 800 nm still showed oil rejection. The explanation can be the same as that when flux was 40 and 60 LMH. Because the fouling in the 200 nm and 400 nm membranes was too severe to run more than 1 cycle, the reversible and irreversible fouling was only calculated for the 600nm membrane experiment and is shown in Figure 14 (d). However, the fouling was dominated by the reversible fouling.

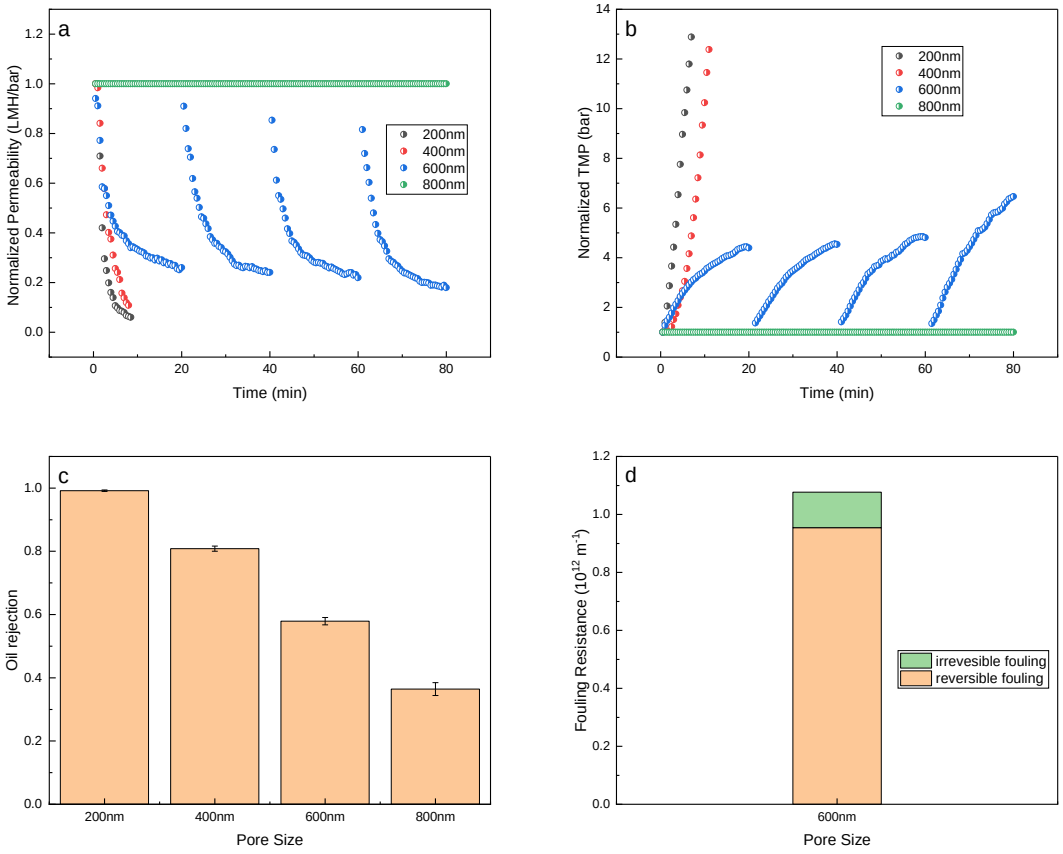

Figure 14. (a) Normalized permeability curve, (b) normalized TMP curve, (c) oil rejection for alumina membranes with different membrane fore sizes filtering 500 mg/L nano-sized O/W emulsions stabilized using Span 80 and Tween 80, (d) reversible and irreversible fouling for 600 nm membranes (flux = 100 LMH)

4.3 Effects of pH

Apart from the pH value, the conditions of the filtration experiments were as follows: 1) cross flow velocity = 0.59 m/s; 2) oil concentration = 500 mg/L; 3) temperature = 20 ± 3˚C; 4) feed flux = 100 LMH; 5) oil droplets mean size = 100 ± 10nm, 6) surfactant concentration = 50 mg/L SDS + 50 mg/L Span 80. The results of the fouling are shown in Figure 15. It can be observed that with the increase in the pH, the decline in normalized permeability became slower and the increase in normalized TMP became slower. This indicates that the increase in pH diminished the membrane fouling. The explanation to this phenomenon could be that with the increase in the

pH, the membrane surface charge became more negative which led to an increased electric repulsion between the oil droplets and the membrane surface as the oil droplets were also negatively charged with the addition of SDS (Contreras et al., 2009; Jones & O'Melia, 2000). The measurement of zeta potential of the feed stream is shown in Figure 16. It can be observed that the pH value had little impact on the zeta potential of the oil droplets, therefore the major contribution of the increase in pH should be that to make the membrane surface became more negatively charged.

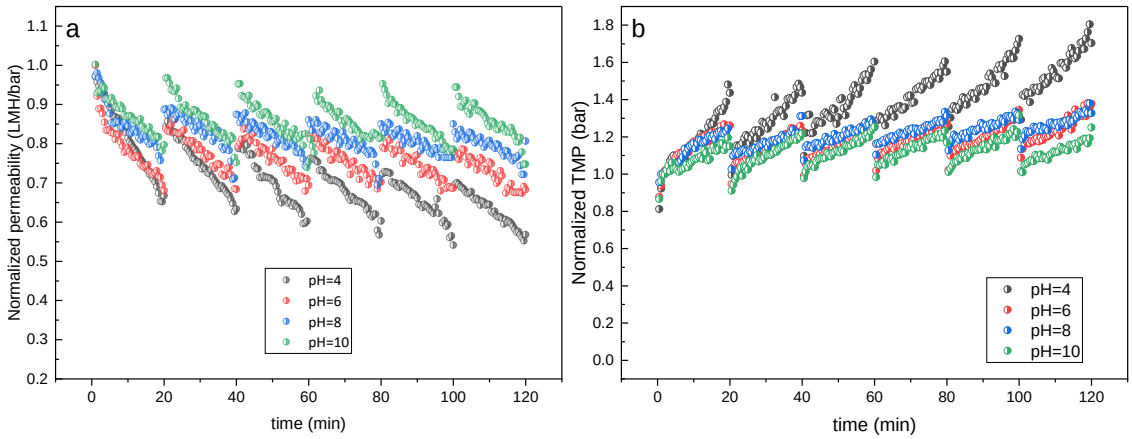

Figure 15. Normalized permeability (a) and TMP (b) curve for different pH value for 100 nm alumina membranes filtering 500 mg/L nano-sized O/W emulsions stabilized using SDS

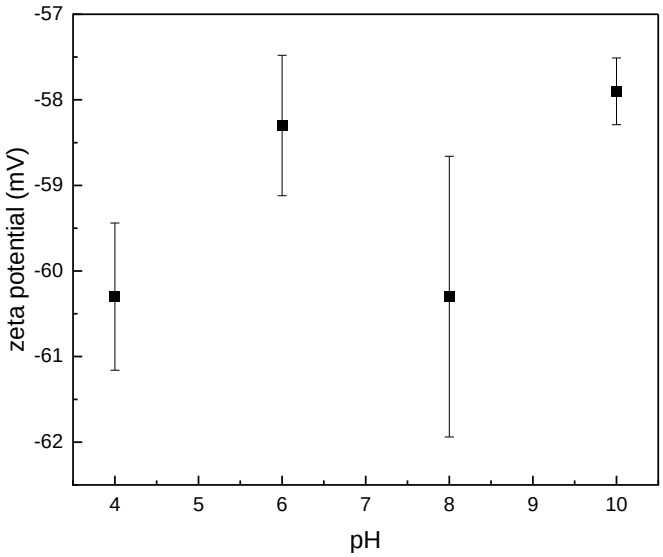

Figure 16. zeta potential of feed streams with different pH values

The irreversible and reversible fouling resistance were calculated and are shown in Figure 17. It was demonstrated that the reversible fouling accounted for a major part of the fouling for all the pH experiments. However, with the increase in pH, reversible fouling became more and more dominant. The reason could be that the electric repulsion between the membrane surface and the oil droplets increased with the pH value and made the oil droplets harder to be deformed. Therefore, the oil droplets became more difficult to be squeezed into the membrane pores and therefore there was less irreversible fouling.

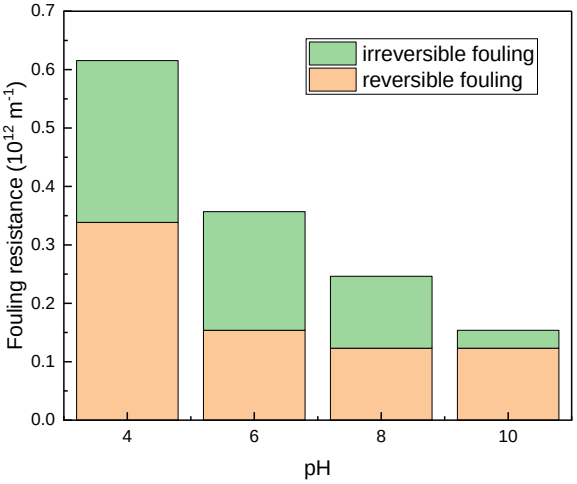

Figure 17. Irreversible and reversible fouling resistance for different pH

4.4 effects of salinity

Apart from the NaCl concentration, the conditions of the filtration experiments were: 1) cross flow velocity = 0.59 m/s; 2) oil concentration = 500 mg/L; 3) temperature = 20 ± 3˚C; 4) feed flux = 100 LMH; 5) oil droplets mean size = 100 ± 10nm, 6) surfactant concentration = 50 mg/L SDS + 50 mg/L Span 80; 7) pH = 5.8. The results of the fouling are shown in Figure 18. It can be observed that with the addition of NaCl from 1mM to 100mM, the fouling became more and more severe. The reason could be that the high ionic strength, resulting from the addition of NaCl, compressed the electrical double layer (EDL) of oil droplets. The zeta potential measurement of the feed stream, shown in Figure 19, became less negative with the increase of NaCl concentration and thus proved the explanation. The compression of EDL led to weaker electric repulsive interaction among oil droplets as well as between oil droplets and membrane surface. The van der Waals forces then dominated the interactions between oil droplets, causing O/W emulsions unstable and promoted aggregation and greater fouling cake formation (Shi et al., 2014). The results agreed with the hypothesis and findings from previous studies.

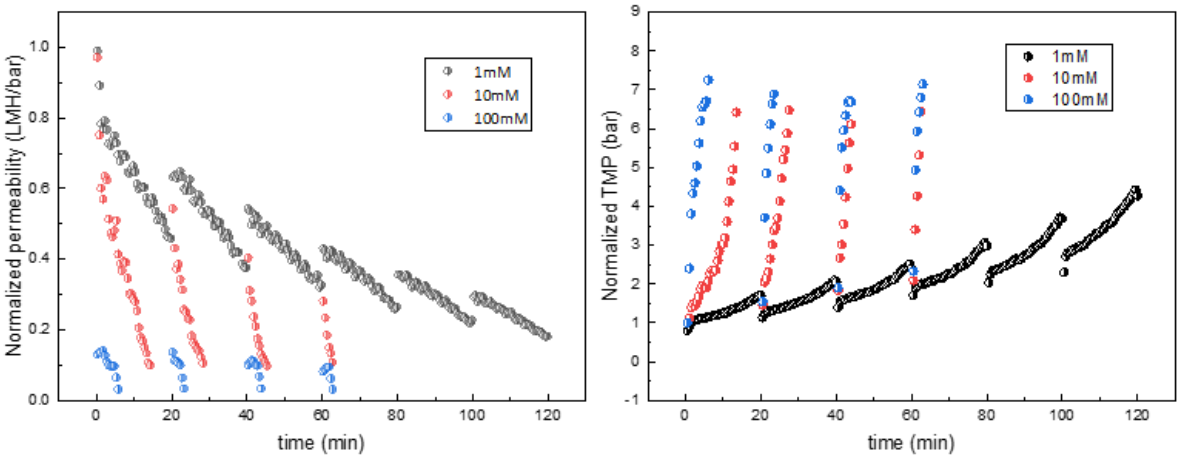

Figure 18. Normalized permeability (a) and TMP (b) curve for different salinity for 100 nm alumina membranes filtering 500 mg/L nano-sized O/W emulsions stabilized using SDS

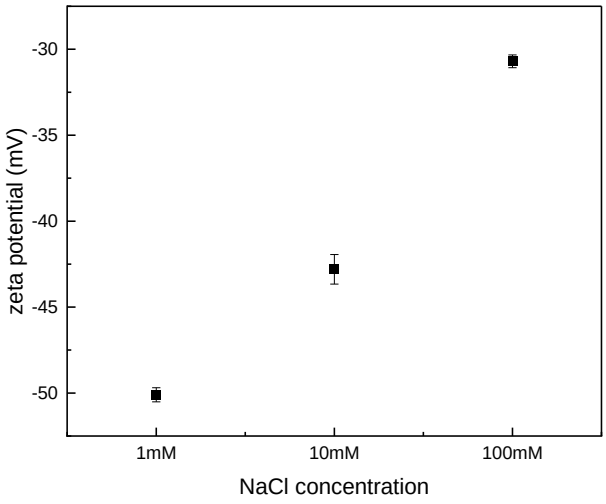

Figure 19. zeta potential of feed streams with different salinity

As shown in Figure 20, with the increase in NaCl concentration, the reversible fouling resistance increased but the irreversible fouling was not influenced much. When the feed stream salinity increased, the permeate flux could not reach the preset constant value. The phenomenon verified the above explanation of the effect of the salinity. With the increase in ionic strength, the nano-sized O/W emulsions became unstable

and oil droplets began to coalescence and resulted in larger droplet size which was shown in Figure 21. Therefore, it was hard to form pore blocking and the cake filtration became dominant.

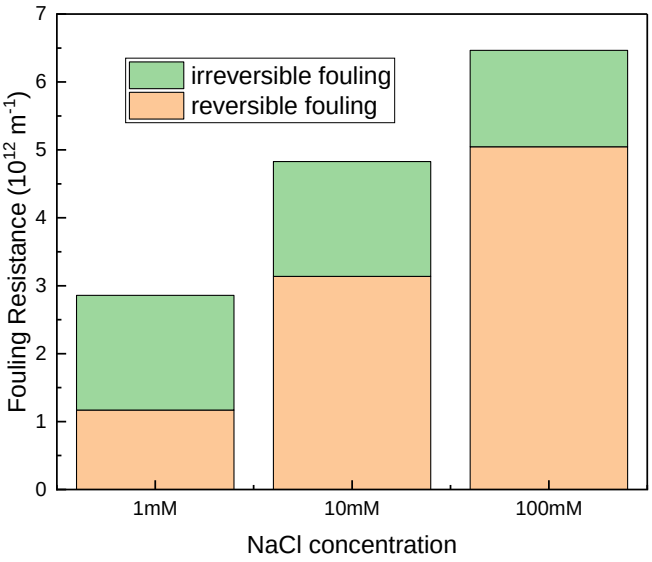

Figure 20. Irreversible and reversible fouling resistance for different salinity

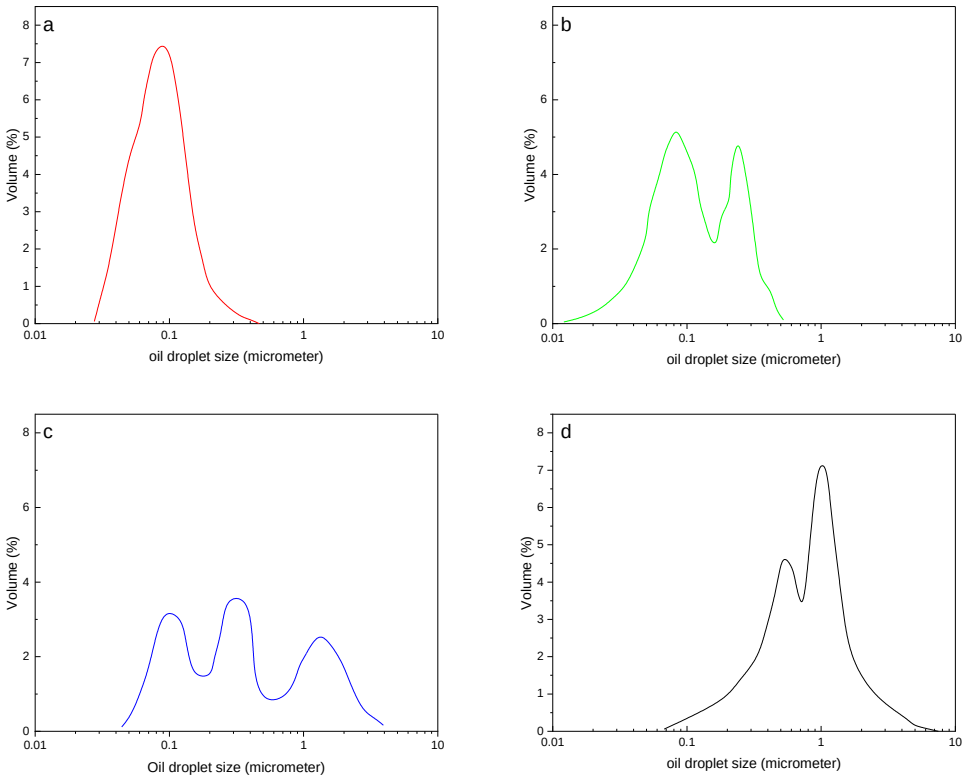

Figure 21. PSD of nano-sized O/W emulsions with different salinity: (a) 0 mM NaCl; (b) 1 mM NaCl; (c) 10mM NaCl; (d) 100 mM NaCl

5. Conclusions

The aim of this thesis was to study the influence of different parameters on the ultrafiltration of nano-sized O/W emulsions using alumina ceramic membranes. The influence of membrane pore size, pH, salinity, and cross flow velocity were investigated as previous studies have shown that they were influential factors, and they were adjustable in real-life separation. Below are the answers to the research questions proposed at the beginning of the thesis.

1) What is the influence of different cross flow velocities on membrane fouling?

   With the increase in cross flow velocities from 0.35 m/s to 0.71 m/s, the shear force near the membrane surface increased and resulted in less deposition of oil droplets. Besides, the turbulent could also lead to coalescence of oil droplets and thereby mitigate the irreversible fouling. It was thus concluded that high cross flow velocities could mitigate the membrane fouling.

2) What is the influence of the membrane pore size (100, 200, 400, 600, 800 nm) on membrane fouling and oil rejection?

   Larger pore sizes result in lower oil rejection and higher permeate flux (Pan, Cao, Li, Du, & Cheng, 2019). Therefore, using membranes with larger pore sizes is thus more economic and efficient. The results showed that when filtrating nano-sized O/W emulsions with an average droplet size of around 100nm (90% < 200nm), alumina membranes with pore sizes of 100 nm could achieve an oil rejection of over 99% and membranes with pore sizes of 200 nm could achieve an oil rejection of over 95%. The oil rejection became increasingly lower when membrane pore sizes increased to 400nm (50% to 75%), 600nm (35% to 60%), and 800nm (30% to 40%). The high oil rejection for the membranes with larger pore sizes could result from the cake layer formed by the coalescence and

aggregation of oil droplets. The fouling resistance was dominated by reversible fouling when the membrane pore sizes were larger, so it was recommended to use 200 nm rather than 100 nm membranes to filtrate nano-sized O/W emulsions.

3) What is the influence of pH on membrane fouling?

   For the negatively charged O/W emulsions, with the increase in pH from 4 to 10, the membrane fouling on alumina membranes were diminished. This was because when pH raised from 4 to 10, the surface charge of alumina membranes became more negative which promoted the electric repulsion between the oil droplets and membrane surface.

4) What is the influence of salinity on membrane fouling?

   For negatively charged O/W emulsions, with the increase in salinity from 1 mM to 100 mM, the membrane fouling on alumina membranes became more severe. The increase in ionic strength in O/W emulsions compressed the EDL of oil droplets resulting in the aggregation of oil droplets and the screening of repulsive interaction between oil droplets and the membrane surfaces. It was concluded that the low salinity condition was favorable to mitigate the membrane fouling.

   .

6. Limitations and recommendations

In this research, there are some limitations due to the time and equipment limits. So, here is some recommendations for future studies:

1) Water / oil contact angle could be measured to determine the hydrophilicity of different membrane pore sizes to better illustrate the interactions between the nano-sized O/W emulsions and the membranes and therefore to explain the high oil rejection.

2) It is good to study the morphology and size of the membrane pores using field emission scanning electron microscopy (SEM, FEI Nova Nano SEM 450, USA) to find out the how the oil droplets get into the membrane pores especially when the oil droplets are smaller than the membrane pores.

3) To better understand the fouling mechanisms during these filtration processes, the development of fouling models is highly suggested, and there are many studies (Field & Wu, 2011; Hwang et al., 2008; Kirschner et al., 2019) working on the combined fouling models which provides examples and guidance. Also, the models can better illustrate the interactions among oil droplets as well as between oil droplets and membranes.

References

Abadi, S. R. H., Sebzari, M. R., Hemati, M., Rekabdar, F., & Mohammadi, T. (2011). Ceramic membrane performance in microfiltration of oily wastewater. *Desalination, 265*(1), 222-228. doi:https://doi.org/10.1016/j.desal.2010.07.055

Amin, S. K., Abdallah, H., Roushdy, M., & El-Sherbiny, S. (2016). An overview of production and development of ceramic membranes. *Int. J. Appl. Eng. Res, 11*(12), 7708-7721.

Baker, R. W. (2012). *Membrane technology and applications*: John Wiley & Sons.

Bayat, A., Mahdavi, H. R., Kazemimoghaddam, M., & Mohammadi, T. (2016). Preparation and characterization of γ-alumina ceramic ultrafiltration membranes for pretreatment of oily wastewater. *Desalination and Water Treatment, 57*(51), 24322-24332. doi:10.1080/19443994.2016.1146922

Beier, S. P., & Jonsson, G. (2010). Critical flux determination by flux-stepping. *AIChE journal, 56*(7), 1739-1747.

Blandin, G., Verliefde, A. R. D., Comas, J., Rodriguez-Roda, I., & Le-Clech, P. (2016). Efficiently Combining Water Reuse and Desalination through Forward Osmosis—Reverse Osmosis (FO-RO) Hybrids: A Critical Review. *Membranes, 6*(3), 37. Retrieved from https://www.mdpi.com/2077-0375/6/3/37

Blanpain-Avet, P., Migdal, J. F., & Bénézech, T. (2009). Chemical cleaning of a tubular ceramic microfiltration membrane fouled with a whey protein concentrate suspension—Characterization of hydraulic and chemical cleanliness. *Journal of Membrane Science, 337*(1), 153-174. doi:https://doi.org/10.1016/j.memsci.2009.03.033

Bolton, G., LaCasse, D., & Kuriyel, R. (2006). Combined models of membrane fouling: Development and application to microfiltration and ultrafiltration of biological fluids. *Journal of Membrane Science, 277*(1), 75-84. doi:https://doi.org/10.1016/j.memsci.2004.12.053

Bowen, W. R., Calvo, J. I., & Hernández, A. (1995). Steps of membrane blocking in flux decline during protein microfiltration. *Journal of Membrane Science, 101*(1), 153-165. doi:https://doi.org/10.1016/0376-7388(94)00295-A

Chang, C. H., Gopalan, R., & Lin, Y. S. (1994). A comparative study on thermal and hydrothermal stability of alumina, titania and zirconia membranes. *Journal of Membrane Science, 91*(1), 27-45. doi:https://doi.org/10.1016/0376-7388(94)00041-7

Chen, K. L., Mylon, S. E., & Elimelech, M. (2006). Aggregation Kinetics of Alginate-Coated Hematite Nanoparticles in Monovalent and Divalent Electrolytes. *Environmental Science & Technology, 40*(5), 1516-1523. doi:10.1021/es0518068

Chen, M., Heijman, S. G. J., Luiten-Olieman, M. W. J., & Rietveld, L. C. (2022). Oil-in-water emulsion separation: Fouling of alumina membranes with and without a silicon carbide deposition in constant flux filtration mode. *Water Research, 216*, 118267. doi:https://doi.org/10.1016/j.watres.2022.118267

Chen, M., Heijman, S. G. J., & Rietveld, L. C. (2021). State-of-the-Art Ceramic Membranes for Oily Wastewater Treatment: Modification and Application. *Membranes, 11*(11). doi:10.3390/membranes11110888

Chen, Y., & Liu, Q. (2020). Progress and Prospects in Membrane Technology for Oil/Water Separation. In *Multidisciplinary Advances in Efficient Separation Processes* (Vol. 1348, pp. 73-87): American Chemical Society.

Cheryan, M., & Rajagopalan, N. (1998). Membrane processing of oily streams. Wastewater treatment and waste reduction. *Journal of Membrane Science, 151*(1), 13-28. doi:https://doi.org/10.1016/S0376-7388(98)00190-2

Choi, K. Y. J., & Dempsey, B. A. (2005). Bench-scale evaluation of critical flux and TMP in low-pressure membrane filtration. *Journal-American Water Works Association, 97*(7), 134-143.

Contreras, A. E., Kim, A., & Li, Q. (2009). Combined fouling of nanofiltration membranes: Mechanisms and effect of organic matter. *Journal of Membrane Science, 327*(1), 87-95. doi:https://doi.org/10.1016/j.memsci.2008.11.030

Cui, J., Zhang, X., Liu, H., Liu, S., & Yeung, K. L. (2008). Preparation and application of zeolite/ceramic microfiltration membranes for treatment of oil contaminated water. *Journal of Membrane Science, 325*(1), 420-426. doi:https://doi.org/10.1016/j.memsci.2008.08.015

de Lint, W. B. S., Benes, N. E., Lyklema, J., Bouwmeester, H. J. M., van der Linde, A. J., & Wessling, M. (2003). Ion Adsorption Parameters Determined from Zeta Potential and Titration Data for a γ-Alumina Nanofiltration Membrane. *Langmuir, 19*(14), 5861-5868. doi:10.1021/la026864a

Dong, B.-B., Wang, F.-H., Yang, M.-Y., Yu, J.-L., Hao, L.-Y., Xu, X., . . . Agathopoulos, S. (2019). Polymer-derived porous SiOC ceramic membranes for efficient oil-water separation and membrane distillation. *Journal of Membrane Science, 579*, 111-119. doi:https://doi.org/10.1016/j.memsci.2019.02.066

Dong, B. Z., Chen, Y., Gao, N. Y., & Fan, J. C. (2006). Effect of pH on UF membrane fouling. *Desalination, 195*(1), 201-208. doi:https://doi.org/10.1016/j.desal.2005.11.012

Fakhru'l-Razi, A., Pendashteh, A., Abdullah, L. C., Biak, D. R., Madaeni, S. S., & Abidin, Z. Z. (2009). Review of technologies for oil and gas produced water treatment. *J Hazard Mater, 170*(2-3), 530-551. doi:10.1016/j.jhazmat.2009.05.044

Field, R. W., & Pearce, G. K. (2011). Critical, sustainable and threshold fluxes for membrane filtration with water industry applications. *Advances in Colloid and Interface Science, 164*(1), 38-44. doi:https://doi.org/10.1016/j.cis.2010.12.008

Field, R. W., & Wu, J. J. (2011). Modelling of permeability loss in membrane filtration: Re-examination of fundamental fouling equations and their link to critical flux. *Desalination, 283*, 68-74. doi:https://doi.org/10.1016/j.desal.2011.04.035

Gao, N., & Xu, Z.-K. (2019). Ceramic membranes with mussel-inspired and nanostructured coatings for water-in-oil emulsions separation. *Separation and Purification Technology, 212*, 737-746. doi:https://doi.org/10.1016/j.seppur.2018.11.084

Gao, W., Liang, H., Ma, J., Han, M., Chen, Z.-l., Han, Z.-s., & Li, G.-b. (2011). Membrane fouling control in ultrafiltration technology for drinking water production: A review. *Desalination, 272*(1), 1-8. doi:https://doi.org/10.1016/j.desal.2011.01.051

Goosen, M., Sablani, S., Al-Hinai, H., Al-Obeidani, S., Al-Belushi, R., & Jackson, a. (2005). Fouling of reverse osmosis and ultrafiltration membranes: a critical review. *Separation science and technology, 39*(10), 2261-2297.

Hammond, E. G., Johnson, L. A., Su, C., Wang, T., & White, P. J. (2005). Soybean oil. *Bailey's industrial oil and fat products*.

Hermia, J. (1982a). Constant pressure blocking filtration laws: application to power-law non-Newtonian fluids. *Institution of chemical Engineers, 60*(3), 183-187.

Hermia, J. (1982b). Constant pressure blocking filtration laws: application to power-law non-Newtonian fluids.

Ho, C.-C., & Zydney, A. L. (2000). A Combined Pore Blockage and Cake Filtration Model for Protein Fouling during Microfiltration. *Journal of Colloid and Interface Science, 232*(2), 389-399. doi:https://doi.org/10.1006/jcis.2000.7231

Hu, L., Gao, S., Ding, X., Wang, D., Jiang, J., Jin, J., & Jiang, L. (2015). Photothermal-Responsive Single-Walled Carbon Nanotube-Based Ultrathin Membranes for On/Off Switchable Separation of Oil-in-Water Nanoemulsions. *ACS Nano, 9*(5), 4835-4842. doi:10.1021/nn5062854

Hu, M.-X., Niu, H.-M., Chen, X.-L., & Zhan, H.-B. (2019). Natural cellulose microfiltration membranes for oil/water nanoemulsions separation. *Colloids and Surfaces A: Physicochemical and Engineering Aspects, 564*, 142-151. doi:https://doi.org/10.1016/j.colsurfa.2018.12.045

Huisman, I. H., Trägårdh, G., Trägårdh, C., & Pihlajamäki, A. (1998). Determining the zeta-potential of ceramic microfiltration membranes using the electroviscous effect. *Journal of Membrane Science, 147*(2), 187-194. doi:https://doi.org/10.1016/S0376-7388(98)00135-5

Hwang, K.-J., Liao, C.-Y., & Tung, K.-L. (2008). Effect of membrane pore size on the particle fouling in membrane filtration. *Desalination, 234*(1), 16-23. doi:https://doi.org/10.1016/j.desal.2007.09.065

Jiang, Q., Zhou, J., Miao, Y., Yang, S., Zhou, M., Zhong, Z., & Xing, W. (2020). Lower-temperature preparation of SiC ceramic membrane using zeolite residue as sintering aid for oil-in-water separation. *Journal of Membrane Science, 610*, 118238. doi:https://doi.org/10.1016/j.memsci.2020.118238

Jones, K. L., & O'Melia, C. R. (2000). Protein and humic acid adsorption onto hydrophilic membrane surfaces: effects of pH and ionic strength. *Journal of Membrane Science, 165*(1), 31-46. doi:https://doi.org/10.1016/S0376-7388(99)00218-5

Jung, S. Y., & Ahn, K. H. (2019). Transport and deposition of colloidal particles on a patterned membrane surface: Effect of cross-flow velocity and the size ratio of particle to surface pattern. *Journal of Membrane Science, 572*, 309-319.

Kajitvichyanukul, P., Hung, Y.-T., & Wang, L. K. (2011). Membrane Technologies for Oil–Water Separation. In L. K. Wang, J. P. Chen, Y.-T. Hung, & N. K. Shammas (Eds.), *Membrane and Desalination Technologies* (pp. 639-668). Totowa, NJ: Humana Press.

Kirschner, A. Y., Cheng, Y.-H., Paul, D. R., Field, R. W., & Freeman, B. D. (2019). Fouling mechanisms in constant flux crossflow ultrafiltration. *Journal of Membrane Science, 574*, 65-75. doi:https://doi.org/10.1016/j.memsci.2018.12.001

Križan Milić, J., Murić, A., Petrinić, I., & Simonič, M. (2013). Recent Developments in Membrane Treatment of Spent Cutting-Oils: A Review. *Industrial & Engineering Chemistry Research, 52*(23), 7603-7616. doi:10.1021/ie4003552

Le Clech, P., Jefferson, B., Chang, I. S., & Judd, S. J. (2003). Critical flux determination by the flux-

step method in a submerged membrane bioreactor. *Journal of Membrane Science, 227*(1-2), 81-93.

Li, D., Huang, X., Huang, Y., Yuan, J., Huang, D., Cheng, G. J., . . . Chang, C. (2019). Additive Printed All-Cellulose Membranes with Hierarchical Structure for Highly Efficient Separation of Oil/Water Nanoemulsions. *ACS Applied Materials & Interfaces, 11*(47), 44375-44382. doi:10.1021/acsami.9b16647

Li, S.-z., & Xu, R.-k. (2008). Electrical double layers' interaction between oppositely charged particles as related to surface charge density and ionic strength. *Colloids and Surfaces A: Physicochemical and Engineering Aspects, 326*(3), 157-161. doi:https://doi.org/10.1016/j.colsurfa.2008.05.023

Lin, Y.-M., & Rutledge, G. C. (2018). Separation of oil-in-water emulsions stabilized by different types of surfactants using electrospun fiber membranes. *Journal of Membrane Science, 563*, 247-258. doi:https://doi.org/10.1016/j.memsci.2018.05.063

Lin, Y. M., Song, C., & Rutledge, G. C. (2019). Functionalization of Electrospun Membranes with Polyelectrolytes for Separation of Oil-In-Water Emulsions. *Advanced Materials Interfaces, 6*(23), 1901285. doi:https://doi.org/10.1002/admi.201901285

Liu, M., Zhu, Z., Zhang, Z., Chu, Y., Yuan, B., & Wei, Z. (2020). Development of highly porous mullite whisker ceramic membranes for oil-in-water separation and resource utilization of coal gangue. *Separation and Purification Technology, 237*, 116483. doi:https://doi.org/10.1016/j.seppur.2019.116483

Miyoshi, T., Yuasa, K., Ishigami, T., Rajabzadeh, S., Kamio, E., Ohmukai, Y., . . . Matsuyama, H. (2015). Effect of membrane polymeric materials on relationship between surface pore size and membrane fouling in membrane bioreactors. *Applied Surface Science, 330*, 351-357. doi:https://doi.org/10.1016/j.apsusc.2015.01.018

Motta Cabrera, S., Winnubst, L., Richter, H., Voigt, I., & Nijmeijer, A. (2021). Industrial application of ceramic nanofiltration membranes for water treatment in oil sands mines. *Separation and Purification Technology, 256*, 117821. doi:https://doi.org/10.1016/j.seppur.2020.117821

Munson, B. R., Okiishi, T. H., Huebsch, W. W., & Rothmayer, A. P. (2013). *Fluid mechanics*: Wiley Singapore.

Nagasawa, H., Omura, T., Asai, T., Kanezashi, M., & Tsuru, T. (2020). Filtration of surfactant-stabilized oil-in-water emulsions with porous ceramic membranes: Effects of membrane pore size and surface charge on fouling behavior. *Journal of Membrane Science, 610*, 118210. doi:https://doi.org/10.1016/j.memsci.2020.118210

Ohshima, H. (2012). The derjaguin-landau-verwey-overbeek (DLVO) theory of colloid stability. *Electrical Phenomena at Interfaces and Biointerfaces: Fundamentals and Applications in Nano-, Bio-, and Environmental Sciences, 27*.

Opawale, F. O., & Burgess, D. J. (2011). Influence of Interfacial Rheological Properties of Mixed Emulsifier Films on the Stability of Water-in-Oil-in-Water Emulsions. *Journal of Pharmacy and Pharmacology, 50*(9), 965-973. doi:10.1111/j.2042-7158.1998.tb06910.x

Pan, Z., Cao, S., Li, J., Du, Z., & Cheng, F. (2019). Anti-fouling TiO2 nanowires membrane for oil/water separation: Synergetic effects of wettability and pore size. *Journal of Membrane Science, 572*, 596-606.

Qin, G. (2021). *The effect of surface charge on threshold flux and fouling behavior of silicon*

carbide membrane with O/W emulsion and sodium alginate solution as typical pollutants. (master). Delft University of Technology, Delft.

Rhee, C., Martyn, P., & Kremer, J. (1987). *Removal of oil and grease in the hydrocarbon processing industry.* Paper presented at the Proceedings 42 nd Industrial Waste Conference. Purdue University.

Shi, X., Tal, G., Hankins, N. P., & Gitis, V. (2014). Fouling and cleaning of ultrafiltration membranes: A review. *Journal of Water Process Engineering, 1*, 121-138. doi:https://doi.org/10.1016/j.jwpe.2014.04.003

Sprycha, R. (1989). Electrical double layer at alumina/electrolyte interface: I. Surface charge and zeta potential. *Journal of Colloid and Interface Science, 127*(1), 1-11. doi:https://doi.org/10.1016/0021-9797(89)90002-7

Tang, C. Y., Chong, T. H., & Fane, A. G. (2011). Colloidal interactions and fouling of NF and RO membranes: A review. *Advances in Colloid and Interface Science, 164*(1), 126-143. doi:https://doi.org/10.1016/j.cis.2010.10.007

Tang, H., Hao, L., Chen, J., Wang, F., Zhang, H., & Guo, Y. (2018). Surface Modification to Fabricate Superhydrophobic and Superoleophilic Alumina Membranes for Oil/Water Separation. *Energy & Fuels, 32*(3), 3627-3636. doi:10.1021/acs.energyfuels.7b03344

Tanudjaja, H. J., Tarabara, V. V., Fane, A. G., & Chew, J. W. (2017). Effect of cross-flow velocity, oil concentration and salinity on the critical flux of an oil-in-water emulsion in microfiltration. *Journal of Membrane Science, 530*, 11-19. doi:https://doi.org/10.1016/j.memsci.2017.02.011

Trägårdh, G. (1989). Membrane cleaning. *Desalination, 71*(3), 325-335. doi:https://doi.org/10.1016/0011-9164(89)85033-7

Tummons, E. N., Tarabara, V. V., Chew, Jia W., & Fane, A. G. (2016). Behavior of oil droplets at the membrane surface during crossflow microfiltration of oil–water emulsions. *Journal of Membrane Science, 500*, 211-224. doi:https://doi.org/10.1016/j.memsci.2015.11.005

Van Gestel, T., Vandecasteele, C., Buekenhoudt, A., Dotremont, C., Luyten, J., Leysen, R., . . . Maes, G. (2002). Alumina and titania multilayer membranes for nanofiltration: preparation, characterization and chemical stability. *Journal of Membrane Science, 207*(1), 73-89. doi:https://doi.org/10.1016/S0376-7388(02)00053-4

Verberk, J., & van Dijk, H. (2003). Research on AirFlush®: distribution of water and air in tubular and capillary membrane modules. *Water Supply, 3*(5-6), 409-414. doi:10.2166/ws.2003.0196

Wang, X., Sun, K., Zhang, G., Yang, F., Lin, S., & Dong, Y. (2022). Robust zirconia ceramic membrane with exceptional performance for purifying nano-emulsion oily wastewater. *Water Research, 208*, 117859. doi:https://doi.org/10.1016/j.watres.2021.117859

Yamamura, H., Kimura, K., & Watanabe, Y. (2007). Mechanism Involved in the Evolution of Physically Irreversible Fouling in Microfiltration and Ultrafiltration Membranes Used for Drinking Water Treatment. *Environmental Science & Technology, 41*(19), 6789-6794. doi:10.1021/es0629054

Yan, L., Li, P., Zhou, W., Wang, Z., Fan, X., Chen, M., . . . Liu, H. (2019). Shrimp Shell-Inspired Antifouling Chitin Nanofibrous Membrane for Efficient Oil/Water Emulsion Separation with In Situ Removal of Heavy Metal Ions. *ACS Sustainable Chemistry & Engineering, 7*(2), 2064-2072. doi:10.1021/acssuschemeng.8b04511

Yang, C., Zhang, G., Xu, N., & Shi, J. (1998). Preparation and application in oil–water separation of ZrO2/α-Al2O3 MF membrane. *Journal of Membrane Science, 142*(2), 235-243. doi:https://doi.org/10.1016/S0376-7388(97)00336-0

Yuan, W., & Zydney, A. L. (2000). Humic acid fouling during ultrafiltration. *Environmental Science and Technology, 34*(23), 5043-5050. doi:10.1021/es0012366

Zhan, H., Zuo, T., Tao, R., & Chang, C. (2018). Robust Tunicate Cellulose Nanocrystal/Palygorskite Nanorod Membranes for Multifunctional Oil/Water Emulsion Separation. *ACS Sustainable Chemistry & Engineering, 6*(8), 10833-10840. doi:10.1021/acssuschemeng.8b02137

Zhong, Z., Xing, W., & Zhang, B. (2013). Fabrication of ceramic membranes with controllable surface roughness and their applications in oil/water separation. *Ceramics International, 39*(4), 4355-4361. doi:https://doi.org/10.1016/j.ceramint.2012.11.019

Zhu, L., Dong, X., Xu, M., Yang, F., Guiver, M. D., & Dong, Y. (2019). Fabrication of mullite ceramic-supported carbon nanotube composite membranes with enhanced performance in direct separation of high-temperature emulsified oil droplets. *Journal of Membrane Science, 582*, 140-150. doi:https://doi.org/10.1016/j.memsci.2019.04.001

Zou, D., Fan, W., Xu, J., Drioli, E., Chen, X., Qiu, M., & Fan, Y. (2021). One-step engineering of low-cost kaolin/fly ash ceramic membranes for efficient separation of oil-water emulsions. *Journal of Membrane Science, 621*, 118954. doi:https://doi.org/10.1016/j.memsci.2020.118954